

Forecasting range shifts of a dioecious plant species under climate change

Jacob K. Moutouama ^{*1}, Aldo Compagnoni², and Tom E.X. Miller¹

¹Program in Ecology and Evolutionary
Biology, Department of BioSciences, Rice University, Houston, TX USA

²Institute
of Biology, Martin Luther University Halle-Wittenberg, Halle, Germany; and
German Centre for Integrative Biodiversity Research (iDiv), Leipzig, Germany

Running header: Forecasting range shifts

Keywords: climate change, demography, forecasting, matrix projection model, mechanistic models, sex ratio, range limits

Acknowledgements: This research was supported by XX.

Authorship statement: XXXXX.

Data accessibility statement: All data (Miller and Compagnoni, 2022a) used in this paper are publicly available. Should the paper be accepted, all computer scripts supporting the results will be archived in a Zenodo package, with the DOI included at the end of the article. During peer review, our data and code are available at <https://github.com/jmoutouama/POAR-Forecasting>.

Conflict of interest statement: None.

^{*}Corresponding author: jmoutouama@gmail.com

1 Abstract

2 Rising temperatures and extreme drought events associated with global climate change have
3 triggered an urgent need for predicting species response to climate change. Currently, the
4 vast majority of theory and models in population biology, including those used to forecast
5 biodiversity responses to climate change ignore the complication of sex structure. To address
6 this issue, we developed two contrasting climate-driven matrix projection models (MPMs),
7 one that account for sex structure and another one that does not account for sex structure.
8 The MPMs were built from demographic data of dioecious species (Texas bluegrass), past and
9 future climate (different carbon gas emission scenarios). Both models predict a sex specific
10 demographic response to climate change. Female individuals have a demographic advantage
11 (higher vital rate) over males. Climate change assuming moderate carbon emission has no
12 negative impact on population viability. However, high carbon emission will likely alter
13 population viability in dioecious species and will induce a North shift in suitable conditions.
14 Overall, our work suggest that tracking only one sex could lead to an underestimation of
15 the impact of climate change on dioecious species. This study provides a framework for
16 predicting the impact of climate on species using population demography.

¹⁷ Introduction

¹⁸ Rising temperatures and extreme drought events associated with global climate change are
¹⁹ leading to increased concern about how species will become redistributed across the globe
²⁰ under future climate conditions (Bertrand et al., 2011; Gamelon et al., 2017; Smith et al., 2024).
²¹ Dioecious species (most animals and many plants) might be particularly vulnerable to the
²² influence of climate change because they often display skewed sex ratios that are generated or
²³ reinforced by sexual niche differentiation (distinct responses of females and males to shared cli-
²⁴ mate drivers) (Tognetti, 2012). Accounting for such a niche differentiation within a population
²⁵ is a long-standing challenge in accurately predicting which sex will successfully track environ-
²⁶ mental change and how this will impact population viability and range shifts (Gissi et al., 2023;
²⁷ Jones et al., 1999). The vast majority of theory and models in population biology, including
²⁸ those used to forecast biodiversity responses to climate change, ignore the complication of sex
²⁹ structure (Ellis et al., 2017; Pottier et al., 2021). As a result, accurate forecasts of colonization-
³⁰ extinction dynamics for dioecious species under future climate scenarios are limited.

³¹ Species's range limits, when not driven by dispersal limitation, should generally reflect
³² the limits of the ecological niche (Lee-Yaw et al., 2016). For most species, niches and geographic
³³ ranges are often limited by climatic factors including temperature and precipitation (Sexton
³⁴ et al., 2009). Therefore, any substantial changes in the magnitude of these climatic factors in a
³⁵ given location across the range could impact population viability, with implications for range
³⁶ shifts based on which regions become more or less suitable (Davis and Shaw, 2001; Pease
³⁷ et al., 1989). Forecasting range shifts for dioecious species is complicated by the potential for
³⁸ each sex to respond differently to climate variation (Morrison et al., 2016; Pottier et al., 2021).
³⁹ Populations in which males are rare under current climatic conditions could experience low
⁴⁰ reproductive success due to sperm or pollen limitation that may lead to population decline in
⁴¹ response to climate change that disproportionately favors females (Eberhart-Phillips et al., 2017).
⁴² In contrast, climate change could expand male habitat suitability (e.g. upslope movement),
⁴³ which might increases seed set for pollen-limited females and favor range expansion (Petry
⁴⁴ et al., 2016). Although the response of species to climate warming is an urgent and active area
⁴⁵ of research, few studies have disentangled the interaction between sex and climate drivers
⁴⁶ to understand their combined effects on population dynamics and range shifts.

⁴⁷ Our ability to track the impact of climate change on the population dynamics of
⁴⁸ dioecious plants and the implication of such impact on range shift depends on our ability
⁴⁹ to build mechanistic models that take into account the spatial and temporal context in which
⁵⁰ sex specific response to climate change affects population viability (Czachura and Miller, 2020;
⁵¹ Davis and Shaw, 2001; Evans et al., 2016). Structured models that are built from long-term

52 demographic data collected from common garden experiments have emerged as powerful
53 technic to study the impact of climate change on species range shift (Merow et al., 2017;
54 Schwinnning et al., 2022). These structured models are increasingly utilized for several reasons.
55 First, structured models enable the manipulation of treatments that can isolate spatial and
56 temporal correlations between environmental factors, thus overcoming a main disadvantage
57 with many types of correlative studies (Leicht-Young et al., 2007). Second, structured models
58 link individual-level demographic trait to population demography allowing the investigation
59 of the demographic mechanisms behind vital rates (e.g. survival, fertility, growth and seed
60 germination) response environmental variation (Dahlgren et al., 2016; Louthan et al., 2022).
61 Third, these structured models can be used to identify which aspect of climate is more
62 important for population dynamics. For example, Life Table Response Experiment (LTRE)
63 build from structured models is an approach that has become widely used to understand
64 how a given treatment (eg. temperature or precipitation) could affect population dynamics
65 (Caswell, 1989; Iler et al., 2019; Morrison and Hik, 2007; O'Connell et al., 2024).

66 In this study, we used a mechanistic approach by combining geographically-distributed
67 field experiments, bayesian statistical modeling, and two-sex population projection modeling
68 to understand the demographic response of dioecious species to climate change and its
69 implications for future range dynamics. Our study system is a dioecious plant species (*Poa*
70 *arachnifera*) distributed along environmental gradients in the south-central US corresponding
71 to variation in temperature across latitude and precipitation across longitude. A previous
72 study on the same system showed that, despite a differentiation of climatic niche between
73 sexes, the female niche mattered the most in driving the environmental limits of population
74 viability (Miller and Compagnoni, 2022b). However that study did not use climate variables
75 preventing us from backcasting and forecasting the impact of climate change on dioecious
76 species. Here, we asked four questions:

- 77 1. What are the sex-specific vital rate responses to variation in temperature and precipitation
78 across the species' range ?
- 79 2. How sex-specific vital rates combine to determine the influence of climate variation on
80 population growth rate (λ) ?
- 81 3. What are the historical and projected changes in climate across the species range ?
- 82 4. What are the back-casted and fore-casted dynamics of this species' geographic niche
83 ($\lambda \geq 1$) and how does accounting for sex structure modify these predictions ?

⁸⁴ **Materials and methods**

⁸⁵ **Study species**

⁸⁶ Texas bluegrass (*Poa arachnifera*) is a dioecious perennial, summer-dormant cool-season (C3)
⁸⁷ grass that occurs in the south-central U.S. (Texas, Oklahoma, and southern Kansas) (Hitchcock,
⁸⁸ 1971). Average temperatures along the distribution of the species tend to decrease northward
⁸⁹ as a result of the influence of latitude: lower latitudes receive more heat from the sun over
⁹⁰ the course of a year. Similarly the average precipitation decrease eastward as a result of
⁹¹ the influence of longitude: lower longitudes receive less precipitation over the year. Texas
⁹² bluegrass grows between October and May (growing season), with onset of dormancy often
⁹³ from June to September (dormant season) (Kindiger, 2004). Flowering occurs in May and
⁹⁴ the species is wind pollinated (Hitchcock, 1971).

⁹⁵ **Common garden experiment**

⁹⁶ We set up a common garden experiment throughout and beyond the range of Texas bluegrass
⁹⁷ to enable study of sex-specific demographic responses to climate and the implications for range
⁹⁸ shifts. The novelty of this study lies in the fact that we use a precise climate variable to build
⁹⁹ a mechanistic model to forecast the response of species to climate change. Details of the exper-
¹⁰⁰ imental design are provided in Miller and Compagnoni (2022b); we provide a brief overview
¹⁰¹ here. The common experiment was installed at 14 sites across a climatic gradient (Fig.1. At
¹⁰² each site, we established 14 blocks. For each block we planted three female and three male indi-
¹⁰³ viduals that were clonally propagated from eight natural source populations of Texas bluegrass.
¹⁰⁴ The experiment was established in November 2013 and was census annually through 2016, pro-
¹⁰⁵ viding both spatial and inter-annual variation in climate. Each May (2014-2016), we collected
¹⁰⁶ individual demographic data including survival (alive or dead), growth (number of tillers),
¹⁰⁷ flowering status (reproductive or vegetative), and fertility (number of panicles, conditional on
¹⁰⁸ flowering). For the analyses that follow, we focus on the 2014-15 and 2015-16 transitions years.

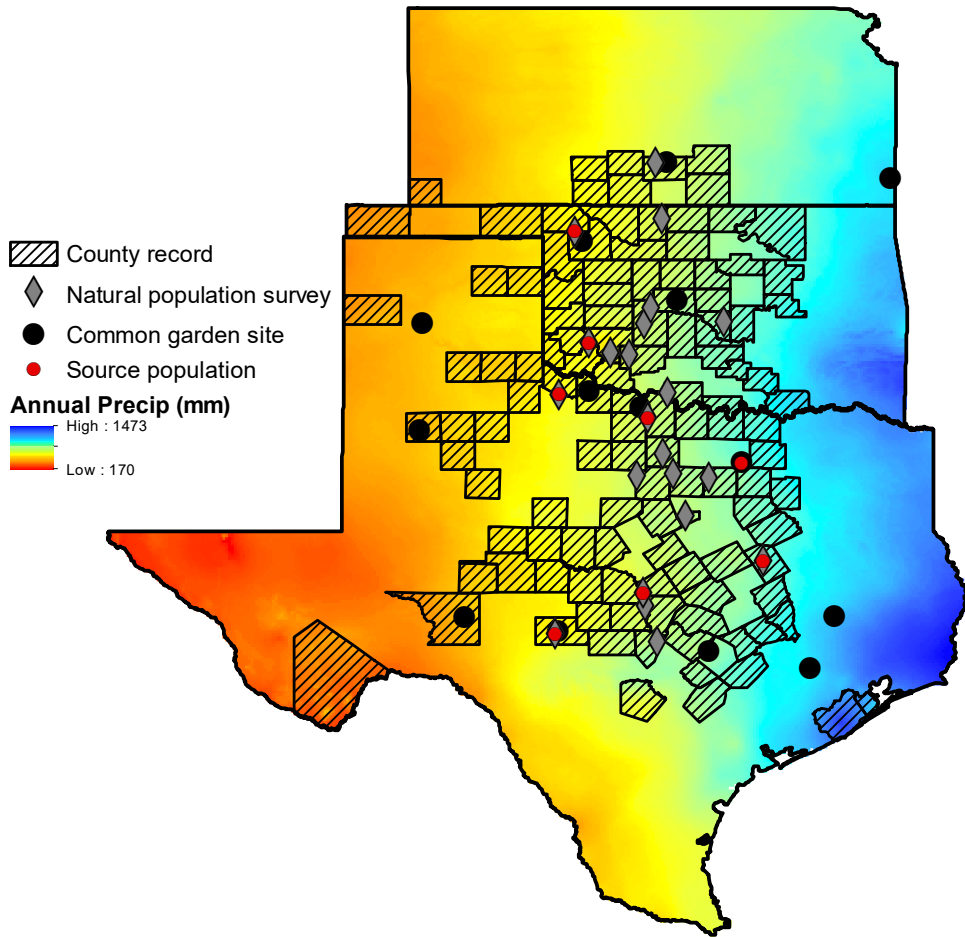


Figure 1: XXX

109 Climatic data collection

110 We downloaded monthly temperature and precipitation from Chelsa to describe observed
 111 climate conditions during our study period (Karger et al., 2017). These climate data were used
 112 as covariates in vital rate regressions, which allowed us to forecast and back-cast demographic
 113 responses to climate change based on observations across the common garden experiment.
 114 We aligned the climatic years to match demographic transition years (**May 1 – April 30**)¹
 115 rather than calendar years. Based on the natural history of this summer-dormant cool-season
 116 species, we divided each transition year into growing and dormant seasons. We define June
 117 through September as the dormant season and the rest of the year as the growing season.

¹I am not sure if these are actually the right dates.

¹¹⁸ Across years and sites, the experiment included substantial variation in growing and dormant
¹¹⁹ season temperature and precipitation (Supporting Information S-1, S-2).

¹²⁰ To back-cast and forecast changes in climate, we downloaded projection data for three
¹²¹ 30-year periods: past (1901-1930), current (1990-2019) and future (2070-2100). Data for these
¹²² climatic periods were downloaded from four general circulation models (GCMs) selected
¹²³ from the Coupled Model Intercomparison Project Phase 5 (CMIP5). The GCMs are MIROC5,
¹²⁴ ACCESS1-3, CESM1-BGC, CMCC-CM and were downloaded from chelsa (Sanderson
¹²⁵ et al., 2015). We evaluated future climate projections from two scenarios of representative
¹²⁶ concentration pathways (RCPs): RCP4.5, an intermediate-to-pessimistic scenario assuming
¹²⁷ a radiative forcing to amount to 4.5 W m^{-2} by 2100, and RCP8.5, a pessimistic emission
¹²⁸ scenario which project a radiative forcing to amount to 8.5 W m^{-2} by 2100 (Schwalm et al.,
¹²⁹ 2020; Thomson et al., 2011).

¹³⁰ Sex ratio experiment

¹³¹ We conducted a sex-ratio experiment on a site close (1 km) to a natural population of the
¹³² focal species at the center of the range to estimate the effect of sex-ratio variation on female
¹³³ reproductive success. Details of the experiment are provided in Compagnoni et al. (2017) and
¹³⁴ Miller and Compagnoni (2022b). In short, we established 124 experimental populations on
¹³⁵ plots measuring $0.4 \times 0.4\text{m}$ and separated by at least 15m from each other at that site. We chose
¹³⁶ 15m because our pilot data show that more than 90% of wind pollination occurred within 13m.
¹³⁷ We varied population density (1-48 plants/plot) and sex ratio (0%-100% female) across the ex-
¹³⁸ perimental populations, and we replicated 34 combinations of density-sex ratios. We collected
¹³⁹ the number of panicles from a subset of females in each plot and collected the number of
¹⁴⁰ seeds in each panicle. Since the number of panicles (proxy of reproduction effort) does not nec-
¹⁴¹ essarily reflect reproduction success in *Poar arachnifera*, we accessed reproduction success (seed
¹⁴² fertilized) using greenhouse-based germination and trazolium-based seed viability assays.

¹⁴³ We used the sex-ratio to estimate the probability of viability and the germination rate.
¹⁴⁴ Seed viability was modeled with a binomial distribution where the probability of viability
¹⁴⁵ (v) was given by:

$$\sup{146} v = v_0 * (1 - OSR^\alpha) \quad (1)$$

¹⁴⁷ where OSR is the operational sex ratio (proportion of panicles that were female) in the
¹⁴⁸ experimental populations. The properties of the above function is supported by our previous
¹⁴⁹ work (Compagnoni et al., 2017). Here, seed viability is maximized at v_0 as OSR approaches

150 zero (strongly male-biased) and goes to zero as *OSR* approaches 1 (strongly female-biased).
151 Parameter α controls how viability declines with increasing female bias.

152 We used a binomial distribution to model the germination data from greenhouse trials.
153 Given that germination was conditional on seed viability, the probability of success was given
154 by the product $v*g$, where v is a function of *OSR* (Eq. 1) and g is assumed to be constant.

155 Sex specific demographic responses to climate

156 We used individual level measurements of survival, growth (number of tillers), flowering, num-
157 ber of panicles to independently develop Bayesian mixed effect models describing how each
158 vital rate varies as a function of sex, size, precipitation of growing and dormant season and tem-
159 perature of of growing and dormant season. We fit vital rate models with second-degree poly-
160 nomial functions for the influence of climate. We included a second-degree polynomial because
161 we expected that climate variables would affect vital rates through a hump-shaped relationship.

162 We centered and standardized all climatic predictors to facilitate model convergence.
163 However, Size was on a natural logarithm scale. We included site,source, and block as
164 random effect. All the vital rate models used the same linear and quadratic predictor for
165 the expected value (μ) (Eq.2) . However, we applied a different link function ($f(\mu)$) depending
166 on the distribution the vital rate. We modeled survival and flowering data with a Bernoulli
167 distribution. We modeled the growth (tiller number) with a zero-truncated Poisson inverse
168 Gaussian distribution. Fertility (panicle count) was model as zero-truncated negative binomial.

$$f(\mu) = \beta_0 + \beta_1 \text{size} + \beta_2 \text{sex} + \beta_3 \text{pptgrow} + \beta_4 \text{pptdorm} + \beta_5 \text{tempgrow} + \beta_6 \text{tempdorm} \\ + \beta_7 \text{pptgrow*sex} + \beta_8 \text{pptdorm*sex} + \beta_9 \text{tempgrow*sex} + \beta_{10} \text{tempdorm*sex} \\ + \beta_{11} \text{size*sex} + \beta_{12} \text{pptgrow*tempgrow} + \beta_{13} \text{pptdorm*tempdorm} \quad (2) \\ + \beta_{14} \text{pptgrow*tempgrow*sex} + \beta_{15} \text{pptdorm*tempdorm*sex} + \beta_{16} \text{pptgrow}^2 \\ + \beta_{17} \text{pptdorm}^2 + \beta_{18} \text{tempgrow}^2 + \beta_{19} \text{tempdorm}^2 + \beta_{20} \text{pptgrow}^2 * \text{sex} \\ + \beta_{21} \text{pptdorm}^2 * \text{sex} + \beta_{22} \text{tempgrow}^2 * \text{sex} + \beta_{23} \text{tempdorm}^2 * \text{sex} + \phi + \rho + \nu$$

170 where β_0 is the grand mean intercept, β_1 is the size dependent slopes. *size* was on a natural log-
171 arithm scale. $\beta_2 \dots \beta_{13}$ represent the climate dependent slopes. $\beta_{14} \dots \beta_{23}$ represent the sex-climate
172 interaction slopes. *pptgrow* is the precipitation of the growing season (standardized to mean
173 zero and unit variance), *tempgrow* is the temperature of the growing season (standardized to
174 mean zero and unit variance), *pptdorm* is the precipitation of the dormant season (standardized
175 to mean zero and unit variance), *tempdorm* is the temperature of the dormant season (standard-
176 ized to mean zero and unit variance). The model also includes normally distributed random ef-

fects for block-to-block variation ($\phi \sim N(0, \sigma_{block})$) and source-to-source variation that is related to the provenance of the seeds used to establish the common garden ($\rho \sim N(0, \sigma_{source})$), site to site variation ($v \sim N(0, \sigma_{site})$). We fit survival, growth, flowering models with generic weakly informative priors for coefficients ($\mu = 0, \sigma = 1.5$) and variances ($\gamma[0.1, 0.1]$). **We fit fertility model with regularizing priors for coefficients ($\mu = 0, \sigma = 0.15$)**. We ran three chains for 1000 samples for warmup and 4000 for interactions, with a thinning rate of 3. We accessed the quality of the models using trace plots and predictive check graphs (Piironen and Vehtari, 2017) (Supporting Information S-4). To understand the effect of climate on vital rates, we got the 95 % credible interval of the posterior distribution. Then we assumed that there is 95 % probability that the true (unknown) estimates would lie within that interval, given the evidence provided by the observed data for each vital rate. All models were fit in Stan (Stan Development Team, 2023).

188 Influence of climate variation on population growth rate

To understand the effect of climate on population growth rate, we used the vital rate estimated earlier to build a matrix projection model (MPM) structured by size (number of tillers), sex and climate (dormant and growing) as covariate. Let $F_{x,z,t}$ and $M_{x,z,t}$ be the number of female and male plants of size x in year t present at a location that has z as climate, where $x \in \{1, 2, \dots, U\}$ and U is the maximum number of tillers a plant can reach (here 95th percentile of observed maximum size). Let F_t^R and M_t^R be the new recruits, which we assume do not reproduce in their first year. We assume that the parameters of sex ratio-dependent mating (Eq. 1) do not vary with climate. For a pre-breeding census, the expected numbers of recruits in year $t+1$ is given by:

$$F_{t+1}^R = \sum_{x=1}^U [p^F(x,z) \cdot c^F(x,z) \cdot d \cdot v(\mathbf{F}_t, \mathbf{M}_t) \cdot m \cdot \rho] F_{x,z,t} \quad (3)$$

$$M_{t+1}^R = \sum_{x=1}^U [p^F(x,z) \cdot c^F(x,z) \cdot d \cdot v(\mathbf{F}_t, \mathbf{M}_t) \cdot m \cdot (1-\rho)] F_{x,z,t} \quad (4)$$

where p^F and c^F are flowering probability and panicle production for females of size x , d is the number of seeds per female panicle, v is the probability that a seed is fertilized, m is the probability that a fertilized seed germinates, and ρ is the primary sex ratio (proportion of recruits that are female), z is the climate. Seed fertilization depends on the OSR of panicles (following Eq. 1) which was derived from the $U \times 1$ vectors of population structure \mathbf{F}_t and \mathbf{M}_t :

$$v(\mathbf{F}_t, \mathbf{M}_t) = v_0 * \left[1 - \left(\frac{\sum_{x=1}^U p^F(x,z) c^F(x,z) F_{x,z,t}}{\sum_{x=1}^U p^F(x,z) c^F(x,z) F_{x,z,t} + p^M(x,z) c^M(x,z) M_{x,z,t}} \right)^\alpha \right] \quad (5)$$

206 Thus, the dynamics of the size-structured component of the population are given by:

207

$$F_{y,t+1} = [\sigma \cdot g^F(y, x=1, z)] F_t^R + \sum_{x=1}^U [s^F(x, z) \cdot g^F(y, x, z)] F_{x,z,t} \quad (6)$$

208

$$M_{y,t+1} = [\sigma \cdot g^M(y, x=1, z)] M_t^R + \sum_{x=1}^U [s^M(x, z) \cdot g^M(y, x, z)] M_{x,z,t} \quad (7)$$

209 In the two formula above, the first term indicates seedlings that survived their first year and en-
210 ter the size distribution of established plants. Instead of using *P. arachnifera* survival probability,
211 we used the seedling survival probability (σ) from demographic studies of the hermaphroditic
212 congener *Poa autumnalis* in east Texas (T.E.X. Miller and J.A. Rudgers, *unpublished data*), and we
213 assume this probability was constant across sexes and climatic variables. We did this because
214 we had little information on the early life cycle transitions of greenhouse-raised transplants.
215 We also assume that $g(y, x=1)$ is the probability that a surviving seedlings reach size y ,
216 the expected future size of 1-tiller plants from the transplant experiment. The second term
217 represents survival and size transition of established plants from the previous year, where
218 s and g give the probabilities of surviving at size x and growing from sizes x to y , respectively,
219 and superscripts indicate that these functions may be unique to females (F) and males (M).

220 Since the two-sex MPM is nonlinear (vital rates affect and are affected by population
221 structure) we estimated the asymptotic geometric growth rate (λ) by numerical simulation,
222 and repeated this across a range of climate.

223 Identifying the mechanisms of population growth rate sensitivity to climate

224 To identify which aspect of climate is most important for population viability, we used
225 a "random design" Life Table Response Experiment (LTRE). We used the RandomForest
226 package to fit a regression model with θ as predictors and λ as response (Ellner et al., 2016;
227 Liaw et al., 2002). The LTRE approximates the variation in λ in response to climate covariates
228 and their interaction (Caswell, 2000; Hernández et al., 2023):

229

$$Var(\lambda_c) \approx \sum_{i=-1}^n \sum_{j=1}^n Cov(\theta_i, \theta_j, \theta_{ij}) + Var(\epsilon) \quad (8)$$

230 where, θ_i , θ_j , θ_{ij} represent respectively the fitted regression slope for the covariates of the
231 dormant season, j the covariates of the growing season and ij the covariates of their interactions.

232 To identify the mechanism by which climate affects population growth rate for each sex,
233 we decomposed the effect of each climate variable (here Climate) on population growth rate (λ)
234 into contribution arising from the effect on each stage-specific vital rate (Caswell, 2000). At this

235 end we used another LTRE with a "regression design". The LTRE with a "regression design" ap-
236 proximates the change in λ with climate as the product of the sensitivity of λ to the parameters
237 times the sensitivity of the parameters to climate, summed over all parameters (Caswell, 1989):

$$238 \quad \frac{\partial \lambda}{\partial \text{climate}} \approx \sum_i \frac{\partial \lambda}{\partial \theta_i^F} \frac{\partial \theta_i^F}{\partial \text{climate}} + \frac{\partial \lambda}{\partial \theta_i^M} \frac{\partial \theta_i^M}{\partial \text{climate}} \quad (9)$$

239 where, θ_i^F and θ_i^M represent sex-specific parameters: the regression coefficients for the
240 intercepts and slopes of size-dependent vital rate functions. Because LTRE contributions are
241 additive, we summed across vital rates to compare the total contributions of female and male
242 parameters.

243 Impact of climate change on niche and range shifts

244 A species' ecological niche can be defined as the range of resources and conditions (physical
245 and environmental) allowing the species to maintain a viable population ($\lambda > 1$). To
246 understand the impact of climate change on species niche shifts, we estimated the probability
247 of population viability being greater than 1, $\Pr(\lambda > 1)$ conditional to two environmental axes:
248 (i) temperature and precipitation of the dormant season and (ii) temperature and precipitation
249 of the growing season. $\Pr(\lambda > 1)$ was calculated using the proportion of the Markov chain
250 Monte Carlo iterations that lead to a $\lambda > 1$ (Diez et al., 2014). $\Pr(\lambda > 1)$ was mapped onto
251 geographic layers of three state (Texas, Oklahoma and Kansas) to delineate past, current and
252 future potential distribution of the species. To do so, we estimated $\Pr(\lambda > 1)$ conditional to
253 all climate covariates for each pixel (1km*1km) across the species range. Because of amount
254 of the computation involve in the Markov chain Monte Carlo iterations, use only 100 posterior
255 samples to estimate $\Pr(\lambda > 1)$ across the Texas, Oklahoma and Kansas.

256 All calculations were processed in parallel using open-source software on the Rice
257 Super computer (NOTS) and the German Centre for Integrative Biodiversity Research (iDiv)
258 High-Performance Computing (HPC) Cluster.

259 Results

260 Sex specific demographic response to climate change

261 Most vital rates were strongly climate dependent, but the magnitude of their response
262 differed between sexes suggesting a sex-specific demographic response to climate. Survival
263 and flowering were strongly more dependent on climate than growth (number of tillers) and

reproduction (number of panicles) (Fig.2; Supporting Information S-5). In addition, we found opposite patterns in the direction of the effect on seasonal climate on the probability of survival and flowering. The growing season (precipitation) has a negative effect on the probability of survival, number of tillers, and the probability of flowering, whereas the dormant season has a positive effect on these vital rates. Unlike precipitation, temperature had different effects on different vital rates. Temperature of the growing season has a positive effect of the probability of survival, a negative effect of the probability of flowering, and the number of tillers, but no significant effect on the number of panicles. Further, there was a female survival and flowering advantage across both climatic seasons (Figures. 3A-3D, 3I-3L). On the contrary, there was a male panicle advantage across all climatic variables (Figure3M-3P). Counter-intuitively, there was no significant sex growth advantage in all season climatic variables (Figures. 3E-3H). Plant size and sex interaction was significant for all vitals rates (Supporting Information S-5). For survival, flowering and reproduction the interaction between temperature and precipitation of the growing season and dormant season was not significant (Supporting Information S-5). However, for growth the interaction between temperature and precipitation of the growing season and dormant season was significantly higher than zero (Supporting Information S-5).

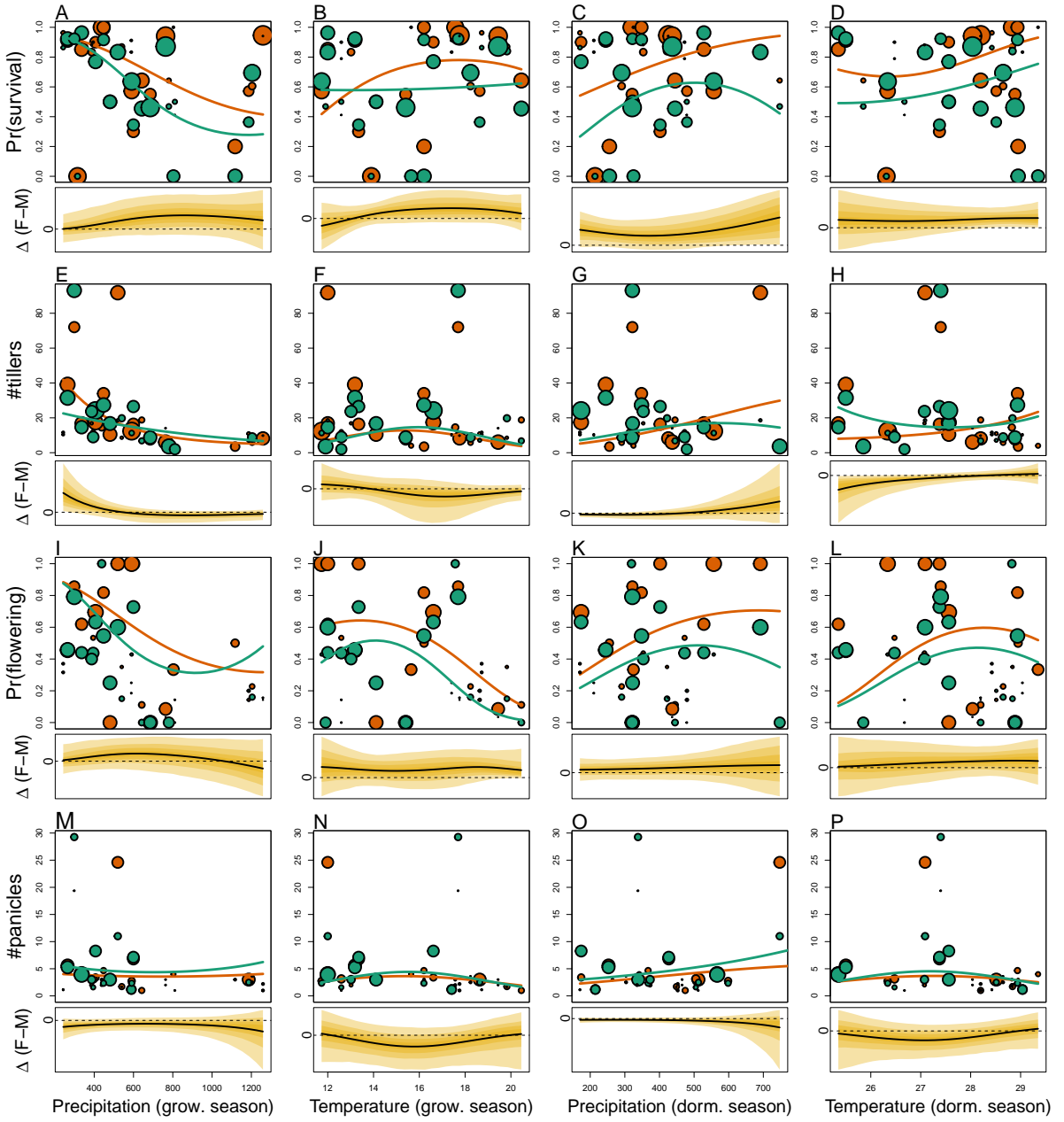


Figure 2: Sex specific demographic response to climate across species range: A–D, seasonal probability of survival; E–H, seasonal growth (change in number of tillers); I–L, seasonal probability of flowering; M–P, number of panicles produced given flowering. Points show means by site for females (orange) and males (green). Point size is proportional to the sample size of the mean. Lines show fitted statistical models for females (orange) and males (green) based on posterior mean parameter values. Lower panels below each data panel show the posterior distribution of the difference between females and males as a function of climate (positive and negative values indicate female and male advantage, respectively); dashed horizontal line shows zero difference.

280 **Climate change alter population viability**

281 We estimated the predicted response of population growth rate (population fitness) to seasonal
282 climate gradients using two models: one accounting for one sex (female dominant) and
283 another one accounting for two sexes. Consistent with the effect of climate on the individual
284 vital rate, we found a strong effect of seasonal climate on population fitness (Fig.3). For both
285 models (female dominant and two sexes), population fitness decreased with an increase of
286 precipitation of growing season. In contrast population fitness increased with precipitation
287 of the dormant season. Furthermore, population fitness was maximized between 23 and 17
288 °C and decreases to zero just beyond 32 °C during the growing season. Similarly population
289 fitness was maximized between 13 and 17 °C and decreases to zero just beyond 20 °C during
290 the growing season. We have also detected a strong effect of the past and future climate on
291 population growth rate. However, the magnitude of the effect of future climate on population
292 growth rate was different between gas-scenario emissions. Under past climate conditions,
293 population growth rate decreased below one for temperature of the growing season. A
294 moderate emission gas scenario (RCP4.5) has a no effect on the population growth rate while
295 a high emission scenario (RCP8.5) has a strong negative effect on population growth rate.

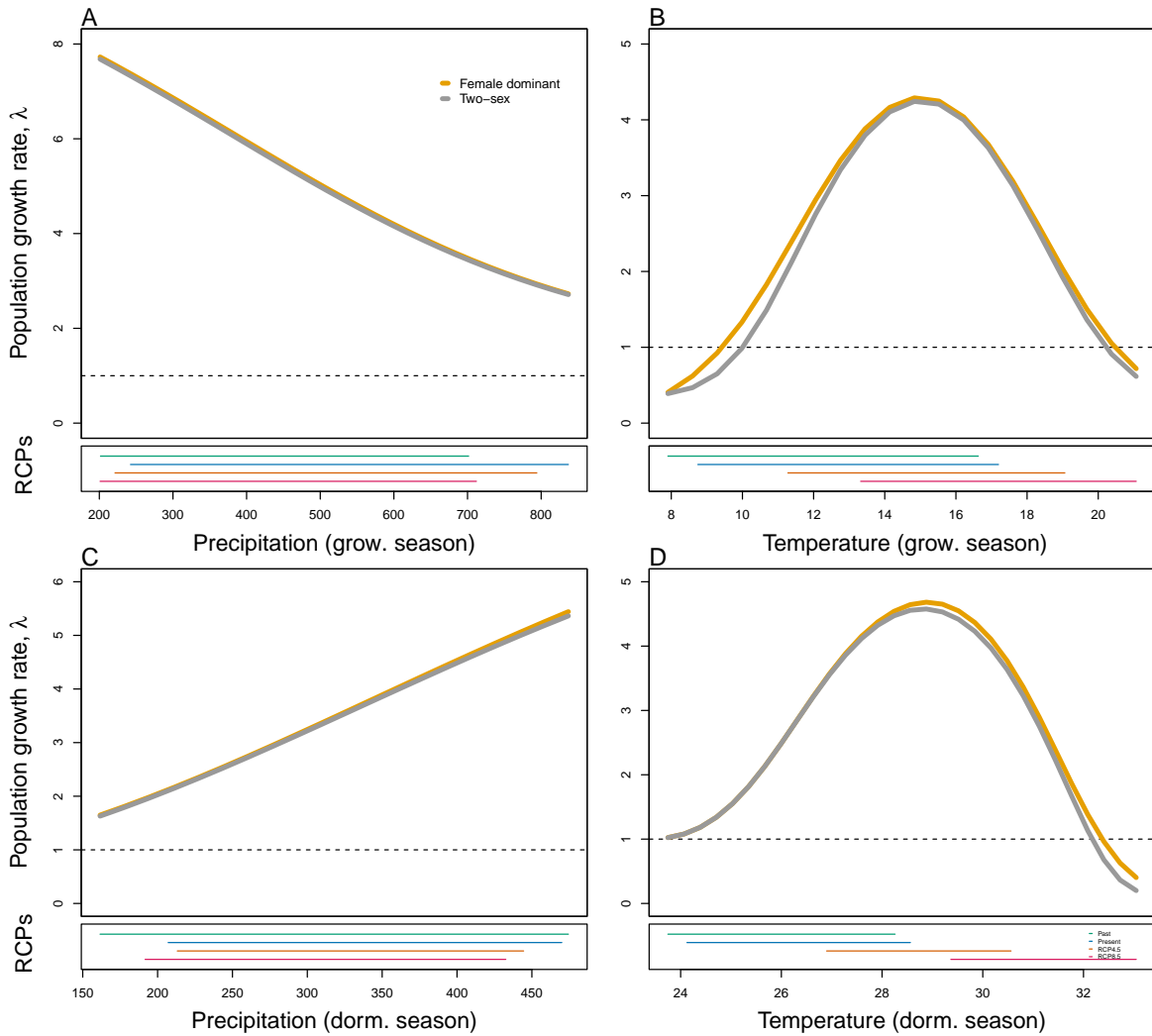


Figure 3: Population growth rate (λ) as a function of climate (past climate, present and predicted future climates). For future climate, we show a Representation Concentration Pathways 4.5 and 8.5. Values of (λ) are derived from the mean climate variables across 4 GCMs. The solid bold curve shows prediction by the two-sex matrix projection model that incorporates sex- specific demographic responses to climate with sex ratio dependent seed fertilization. The bold dashed curve represents the prediction by the female dominant matrix projection model. The dashed horizontal line indicates the limit of population viability ($\lambda = 1$)

296 Temperature as a driver of population viability decline

297 Population viability was most sensitive to change in temperature of the growing season and
 298 temperature of the dormant season (Supporting Information S-10). LTRE decomposition
 299 reveals that, for each sex, the reduction of lambda for high value of temperature of the
 300 growing season was driven by a reduction of survival rate, growth rate, flowering and a

301 reduction in number of panicles. However, the reduction of for higher value of temperature
 302 of the dormant season was driven by only the female.

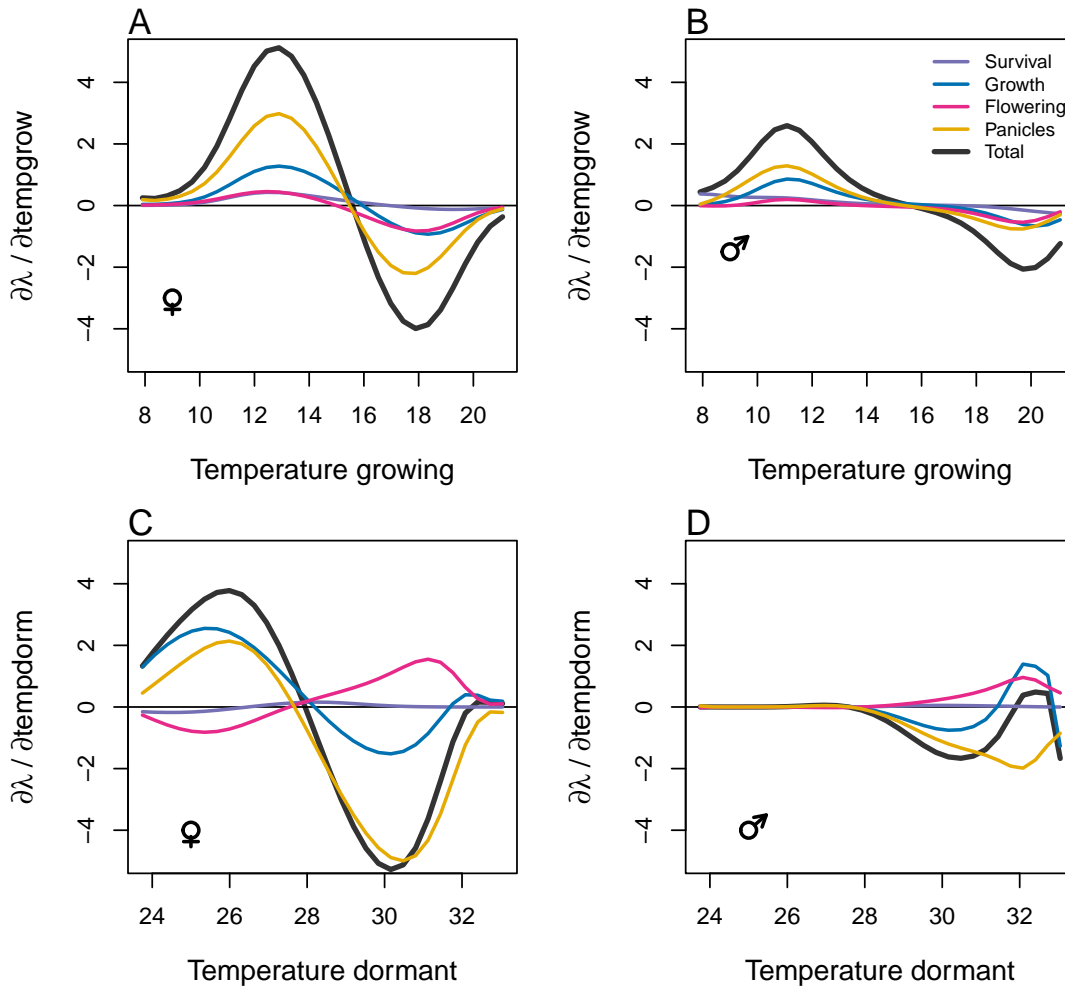


Figure 4: XXX

303 Climatic change induce range shifts

304 Across species niche population persistence was maximized at higher temperature during the
 305 dormant season (27 to 31) and intermediate temperature during the growing season (11 to
 306 20). Our demographically based range predictions broadly captured the known distribution
 307 of the species (Fig. 1). More specifically, the predicted population viable ($\lambda > 1$) matches

308 the presence and absence of the species. Furthermore, viable populations of *P. arichnifera*
309 were only predicted at the center of the range for current climatic conditions (Fig1). Future
310 and past projections of climate change showed a north-west range shift compared to current
311 distributions. Although *P. arichnifera* was predicted to have suitable habitat in the center of the
312 range under the current climate, future warming is predicted to reduce much of the suitable
313 habitat in the southern part (Figure).

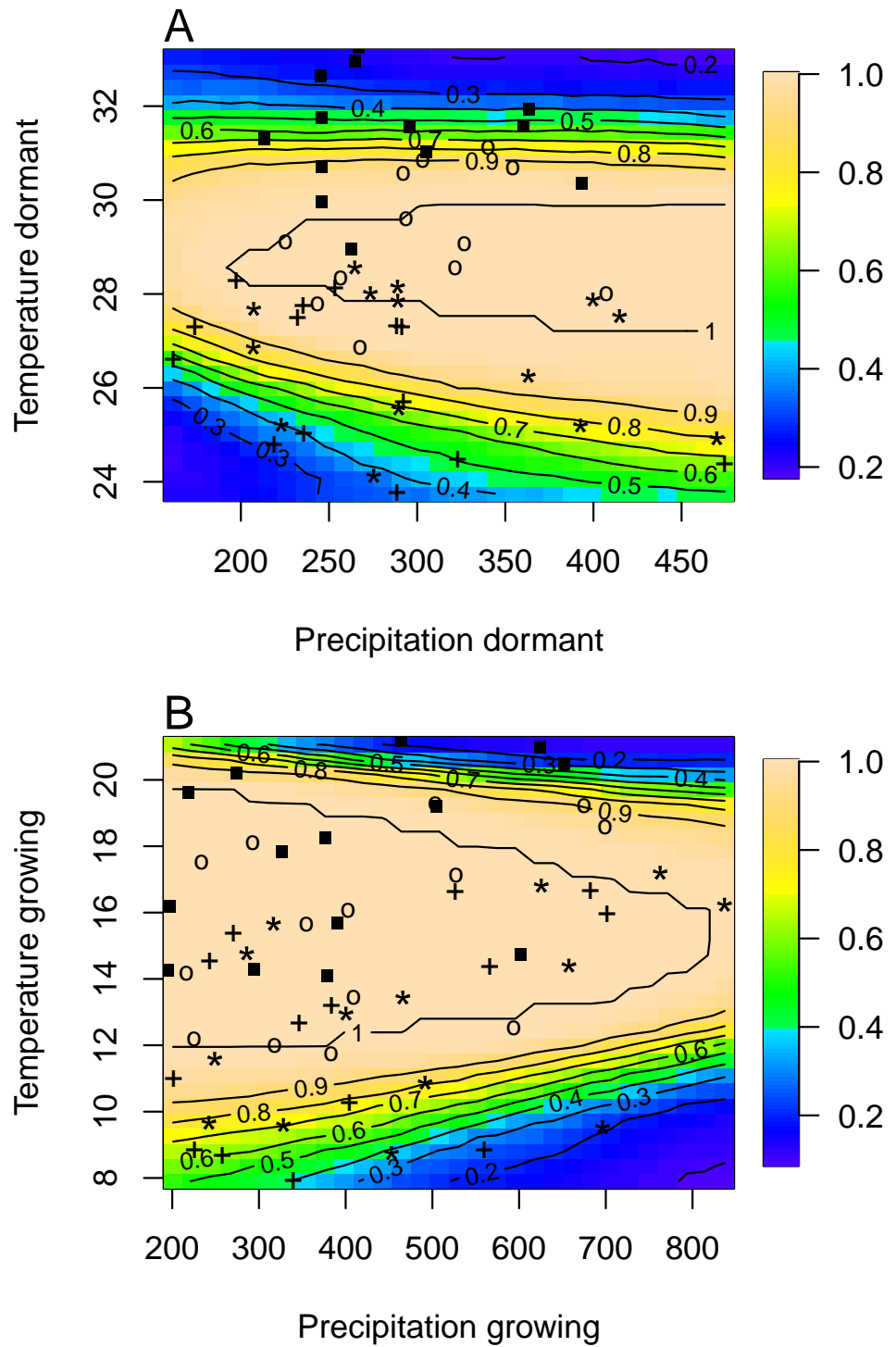


Figure 5: Predicted niche shift for past, present and future climate conditions based on $\text{Pr} (\lambda \geq 1)$. Niche of dormant season (A), Niche of growing season (B). Contours show predicted probabilities of self-sustaining populations $\text{Pr} (\lambda \geq 1)$ conditional on precipitation and temperature of the dormant and growing season."+" Past, "*" Current,"o" RCP 45,"." RCP 85

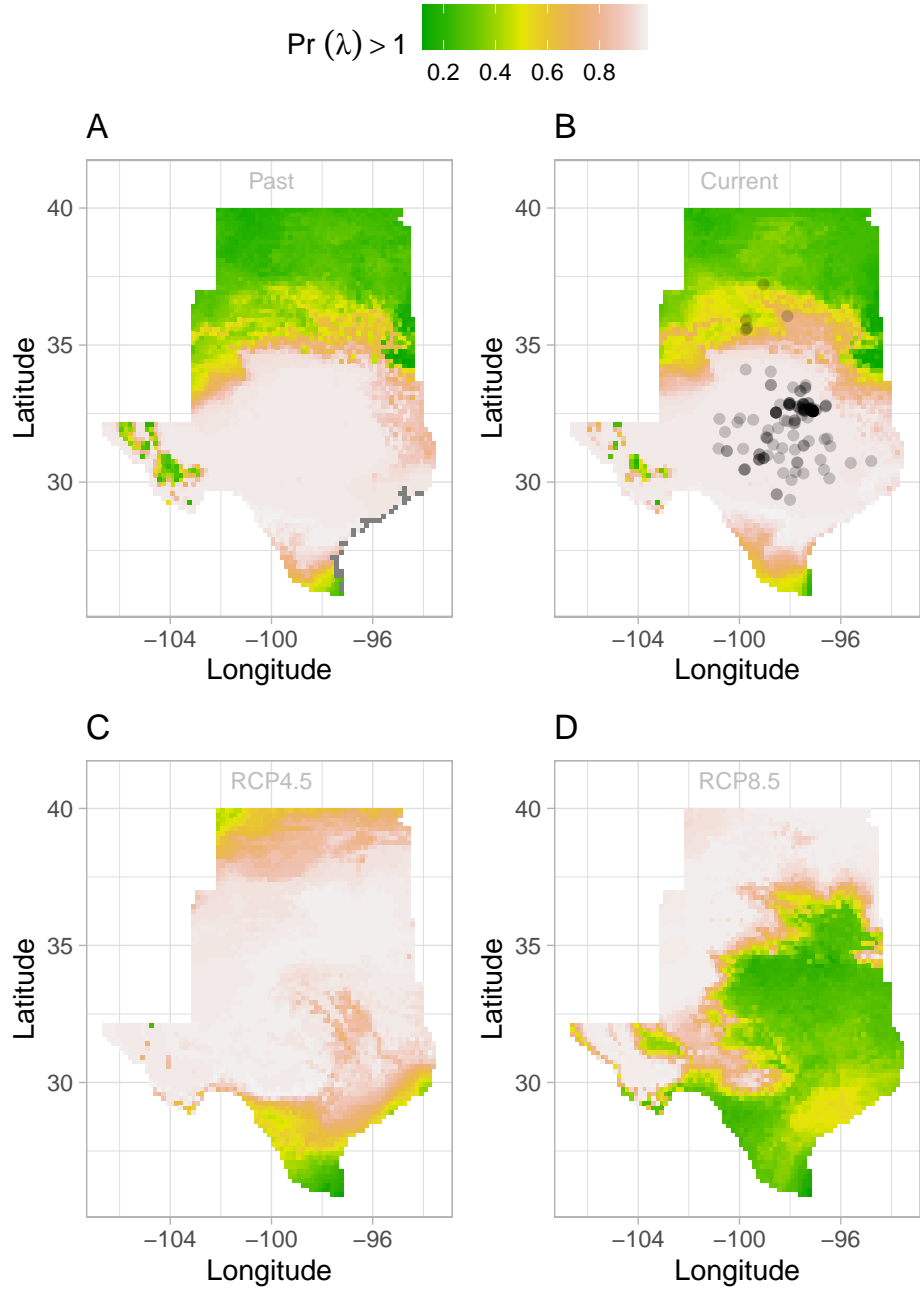


Figure 6: Past (A), Current (B), Future (2070–20100) (C and D) predicted range shift based on population growth rate using the two sex model. Future projections were based on MIROC. The black circles on panel B indicate all known presence points collected from GBIF from 1990 to 2019, which corresponds to the current condition in our prediction. The occurrences of GBIFs are distributed in with higher population fitness habitat ($\lambda > 1$), confirming that our study approach can reasonably predict range shifts.

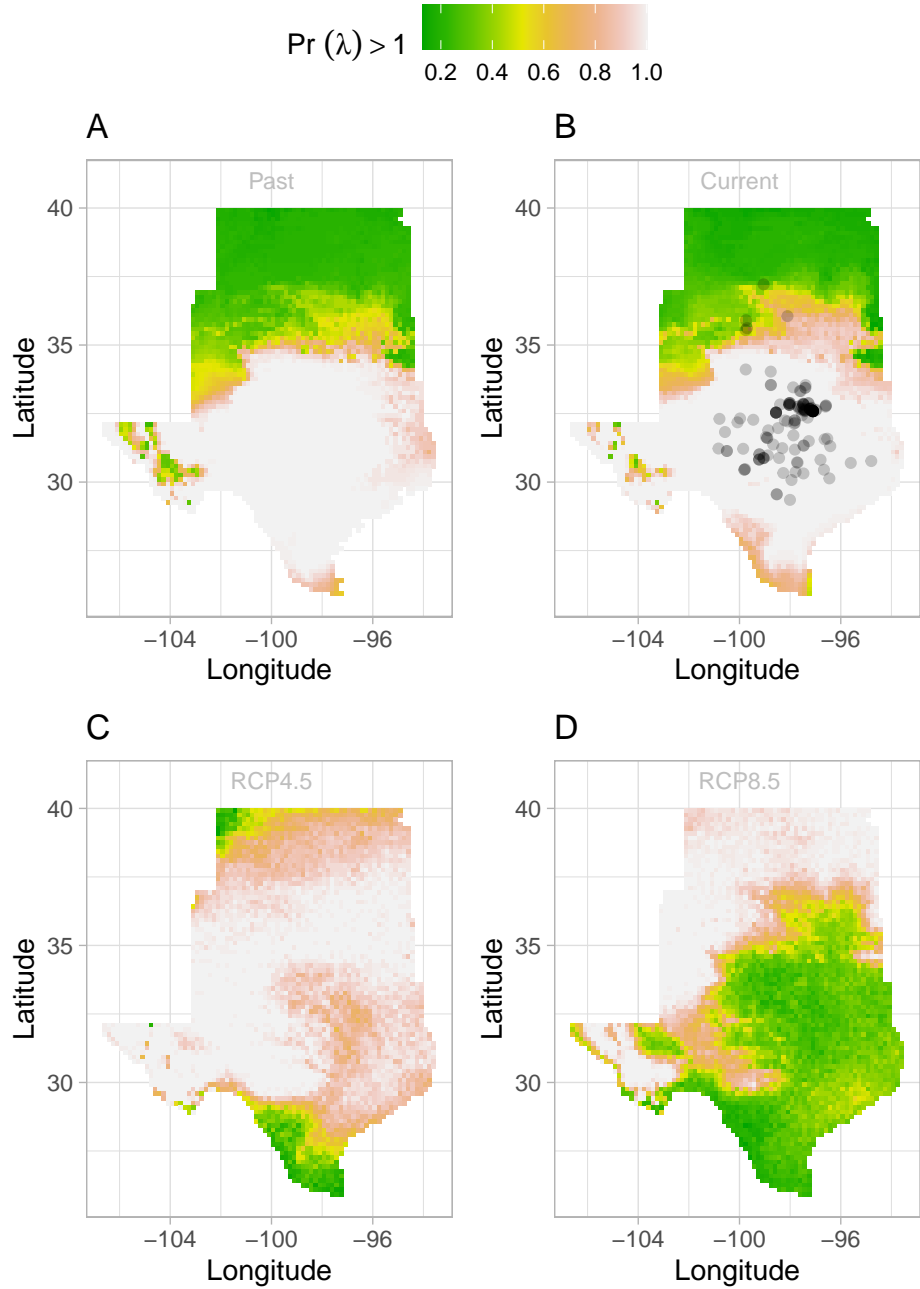


Figure 7: Past (A), Current (B), Future (2070–20100) (C and D) predicted range shift based on population growth rate using the female dominant model. Future projections were based on the average population growth rate in four GCMs. The black circles on panel B indicate all known presence points collected from GBIF from 1990 to 2019, which corresponds to the current condition in our prediction. The occurrences of GBIFs are distributed in with higher population fitness habitat ($\lambda > 1$), confirming that our study approach can reasonably predict range shifts.

314 **Discussion**

315 Three general patterns emerged from our analysis. First, our Bayesian mixed effect model
316 predicts that seasonal climate (temperature and precipitation) affects sex-demographic
317 processes in distinctive and contrasting ways. While climate has a significant effect on the
318 probability of survival and growth, it has no effect on the number of panicles. Second, future
319 climate, by increasing seasonal temperature, will lead to decline in population viability and
320 favor range shifts. Third, using only one sex to forecast range shifts of dioecious under climate
321 change could lead to an underestimation of the impact of climate change on species.

322 Our results indicate a sex-specific demographic response to climate change. Females
323 have higher survival rate and fertility rate than males. This result is not unique to our study
324 system and has been observed in a range of abiotic pollen dispersal species across climatic
325 gradients (Sasaki et al., 2019; Welbergen et al., 2008; Zhao et al., 2012). Several hypotheses
326 could explain the observed demographic advantage of females over males for survival and
327 flowering and the opposite for growth and number of panicles. First, the trade-off between
328 fitness traits (survival, growth, fertility) due to resource limitation and the pollination mode
329 of our study species (wind pollinated) could explain such a result (Cipollini and Whigham,
330 1994; Freeman et al., 1976). For most species, females often pay more for reproduction than
331 males due to the requirement to develop seeds and fruits (Hultine et al., 2016). However,
332 several studies reported a higher cost of reproduction for males in wind pollinated species
333 due to the larger amounts of pollen they produce (Bruijning et al., 2017; Bürli et al., 2022;
334 Cipollini and Whigham, 1994; Field et al., 2013). In addition to life history trade-off, other
335 among site difference in non-climatic factors such as soil, or biotic interactions could explain
336 decline in vital rate as an indirect effect of increase in temperature (Alexander et al., 2015).

337 Under current conditions, most populations across the range are viable. This result could
338 be explained by two hypotheses. First, demographic compensation whereby an increase of
339 one vital rate is coupled with a decrease of another vital rate could explain a viable population
340 in harsh conditions at the range edge (Doak and Morris, 2010; Nomoto and Alexander, 2021;
341 Villegas et al., 2015). In our system, a decrease in fertility survival rate was counterbalanced
342 by an increase in survival rate, preventing the population growth rate from declining even
343 at range edge for the growing season. Second, local adaptation at the edge of the range could
344 explain the viable population throughout the range (Miller and Compagnoni, 2022b). Our
345 study was based on a common garden experiment; therefore, individuals planted in climatic
346 conditions that are similar to their source populations climatic conditions were less impacted
347 by stressful environmental conditions. One important question to ask is: what is the role
348 of local adaptation in buffering species response to climate change. Adding another predictor

349 to our complex model would have lead to overfitting. Therefore, our model does not shed
350 light on the importance of local adaptation in species response to climate change. The role
351 of local adpatation in mitigating population response to climate should be the next step in
352 forecasting species response to climate.

353 Our LTRE analysis reveals that a small changes in temperature of the growing and
354 dormant season could have a larger impact on population viability. This results suggest
355 that projected future climate will affect population viability. Temperature can impact plant
356 populations through different mechanisms. Increasing temperature could increase evaporative
357 demand, affect plant phenology (Dolschak et al., 2019), and germination rate (Reed et al.,
358 2021). The potential for temperature to influence these different processes changes seasonally
359 (Konapala et al., 2020). In the summer growing season, when the temperature is high, the effect
360 on the water balance should be strong (Adler and HilleRisLambers, 2008). In the dormant
361 season, when evaporative demand is low, temperature should have a more important effect
362 on phenology and germination. Because our study species was sensitive to temperatures in
363 the growing season, the former mechanism deserve further attention. Three years represent a
364 relatively decent time for demographic study for common garden experiments across climatic
365 gradient, it can only capture a certain range of demographic and environmental variability.
366 Moreover, our future projections require extrapolation to warmer or colder conditions than
367 observed in our experiment and subsequently should be interpreted with caution. Although
368 our climate-driven projection matrix models may not be perfect when extrapolating, the qual-
369 iitative implications of a negative response of the species to increase temperature (dormant and
370 growing season) seems consistent across all climate all GCMs. Our work suggest that current
371 climate may not affect population viability, but populations may be impacted negatively over
372 the next year in response to a climate change. This is key because most conservation actions
373 are design from data on current responses to climate, rather than future response to climate

374 The reduction in population viability across the range due to climate change will drive
375 a shift to the north range in suitable habitat for the species.

376 **References**

- 377 Adler, P. B. and HilleRisLambers, J. (2008). The influence of climate and species composition
378 on the population dynamics of ten prairie forbs. *Ecology*, 89(11):3049–3060.
- 379 Alexander, J. M., Diez, J. M., and Levine, J. M. (2015). Novel competitors shape species'
380 responses to climate change. *Nature*, 525(7570):515–518.
- 381 Bertrand, R., Lenoir, J., Piedallu, C., Riofrío-Dillon, G., De Ruffray, P., Vidal, C., Pierrat, J.-C.,
382 and Gégout, J.-C. (2011). Changes in plant community composition lag behind climate
383 warming in lowland forests. *Nature*, 479(7374):517–520.
- 384 Bruijning, M., Visser, M. D., Muller-Landau, H. C., Wright, S. J., Comita, L. S., Hubbell, S. P.,
385 de Kroon, H., and Jongejans, E. (2017). Surviving in a cosexual world: A cost-benefit
386 analysis of dioecy in tropical trees. *The American Naturalist*, 189(3):297–314.
- 387 Bürli, S., Pannell, J. R., and Tonnabel, J. (2022). Environmental variation in sex ratios and
388 sexual dimorphism in three wind-pollinated dioecious plant species. *Oikos*, 2022(6):e08651.
- 389 Caswell, H. (1989). Analysis of life table response experiments i. decomposition of effects
390 on population growth rate. *Ecological Modelling*, 46(3-4):221–237.
- 391 Caswell, H. (2000). *Matrix population models*, volume 1. Sinauer Sunderland, MA.
- 392 Cipollini, M. L. and Whigham, D. F. (1994). Sexual dimorphism and cost of reproduction
393 in the dioecious shrub *lindera benzoin* (lauraceae). *American Journal of Botany*, 81(1):65–75.
- 394 Compagnoni, A., Steigman, K., and Miller, T. E. (2017). Can't live with them, can't live
395 without them? balancing mating and competition in two-sex populations. *Proceedings of
396 the Royal Society B: Biological Sciences*, 284(1865):20171999.
- 397 Czachura, K. and Miller, T. E. (2020). Demographic back-casting reveals that subtle
398 dimensions of climate change have strong effects on population viability. *Journal of Ecology*,
399 108(6):2557–2570.
- 400 Dahlgren, J. P., Bengtsson, K., and Ehrlén, J. (2016). The demography of climate-driven and
401 density-regulated population dynamics in a perennial plant. *Ecology*, 97(4):899–907.
- 402 Davis, M. B. and Shaw, R. G. (2001). Range shifts and adaptive responses to quaternary
403 climate change. *Science*, 292(5517):673–679.

- 404 Diez, J. M., Giladi, I., Warren, R., and Pulliam, H. R. (2014). Probabilistic and spatially variable
405 niches inferred from demography. *Journal of ecology*, 102(2):544–554.
- 406 Doak, D. F. and Morris, W. F. (2010). Demographic compensation and tipping points in
407 climate-induced range shifts. *Nature*, 467(7318):959–962.
- 408 Dolschak, K., Gartner, K., and Berger, T. W. (2019). The impact of rising temperatures on
409 water balance and phenology of european beech (*fagus sylvatica l.*) stands. *Modeling earth*
410 *systems and environment*, 5:1347–1363.
- 411 Eberhart-Phillips, L. J., Küpper, C., Miller, T. E., Cruz-López, M., Maher, K. H., Dos Remedios,
412 N., Stoffel, M. A., Hoffman, J. I., Krüger, O., and Székely, T. (2017). Sex-specific early
413 survival drives adult sex ratio bias in snowy plovers and impacts mating system and
414 population growth. *Proceedings of the National Academy of Sciences*, 114(27):E5474–E5481.
- 415 Ellis, R. P., Davison, W., Queirós, A. M., Kroeker, K. J., Calosi, P., Dupont, S., Spicer, J. I.,
416 Wilson, R. W., Widdicombe, S., and Urbina, M. A. (2017). Does sex really matter? explaining
417 intraspecies variation in ocean acidification responses. *Biology letters*, 13(2):20160761.
- 418 Ellner, S. P., Childs, D. Z., Rees, M., et al. (2016). Data-driven modelling of structured
419 populations. *A practical guide to the Integral Projection Model*. Cham: Springer.
- 420 Evans, M. E., Merow, C., Record, S., McMahon, S. M., and Enquist, B. J. (2016). Towards
421 process-based range modeling of many species. *Trends in Ecology & Evolution*, 31(11):860–871.
- 422 Field, D. L., Pickup, M., and Barrett, S. C. (2013). Comparative analyses of sex-ratio variation
423 in dioecious flowering plants. *Evolution*, 67(3):661–672.
- 424 Freeman, D. C., Klikoff, L. G., and Harper, K. T. (1976). Differential resource utilization by
425 the sexes of dioecious plants. *Science*, 193(4253):597–599.
- 426 Gamelon, M., Grøtan, V., Nilsson, A. L., Engen, S., Hurrell, J. W., Jerstad, K., Phillips, A. S.,
427 Røstad, O. W., Slagsvold, T., Walseng, B., et al. (2017). Interactions between demography
428 and environmental effects are important determinants of population dynamics. *Science Advances*, 3(2):e1602298.
- 430 Gissi, E., Schiebinger, L., Hadly, E. A., Crowder, L. B., Santoleri, R., and Micheli, F. (2023).
431 Exploring climate-induced sex-based differences in aquatic and terrestrial ecosystems to
432 mitigate biodiversity loss. *nature communications*, 14(1):4787.

- 433 Hernández, C. M., Ellner, S. P., Adler, P. B., Hooker, G., and Snyder, R. E. (2023). An exact
434 version of life table response experiment analysis, and the r package exactltre. *Methods*
435 in Ecology and Evolution, 14(3):939–951.
- 436 Hitchcock, A. S. (1971). *Manual of the grasses of the United States*, volume 2. Courier Corporation.
- 437 Hultine, K. R., Grady, K. C., Wood, T. E., Shuster, S. M., Stella, J. C., and Whitham, T. G. (2016).
438 Climate change perils for dioecious plant species. *Nature Plants*, 2(8):1–8.
- 439 Iler, A. M., Compagnoni, A., Inouye, D. W., Williams, J. L., CaraDonna, P. J., Anderson, A., and
440 Miller, T. E. (2019). Reproductive losses due to climate change-induced earlier flowering are
441 not the primary threat to plant population viability in a perennial herb. *Journal of Ecology*,
442 107(4):1931–1943.
- 443 Jones, M. H., Macdonald, S. E., and Henry, G. H. (1999). Sex-and habitat-specific responses
444 of a high arctic willow, *salix arctica*, to experimental climate change. *Oikos*, pages 129–138.
- 445 Karger, D. N., Conrad, O., Böhner, J., Kawohl, T., Kreft, H., Soria-Auza, R. W., Zimmermann,
446 N. E., Linder, H. P., and Kessler, M. (2017). Climatologies at high resolution for the earth’s
447 land surface areas. *Scientific data*, 4(1):1–20.
- 448 Kindiger, B. (2004). Interspecific hybrids of *poa arachnifera* × *poa secunda*. *Journal of New*
449 *Seeds*, 6(1):1–26.
- 450 Konapala, G., Mishra, A. K., Wada, Y., and Mann, M. E. (2020). Climate change will affect
451 global water availability through compounding changes in seasonal precipitation and
452 evaporation. *Nature communications*, 11(1):3044.
- 453 Lee-Yaw, J. A., Kharouba, H. M., Bontrager, M., Mahony, C., Csergő, A. M., Noreen, A. M.,
454 Li, Q., Schuster, R., and Angert, A. L. (2016). A synthesis of transplant experiments and
455 ecological niche models suggests that range limits are often niche limits. *Ecology letters*,
456 19(6):710–722.
- 457 Leicht-Young, S. A., Silander, J. A., and Latimer, A. M. (2007). Comparative performance of
458 invasive and native *celastrus* species across environmental gradients. *Oecologia*, 154:273–282.
- 459 Liaw, A., Wiener, M., et al. (2002). Classification and regression by randomforest. *R news*,
460 2(3):18–22.
- 461 Louthan, A. M., Keighron, M., Kiekebusch, E., Cayton, H., Terando, A., and Morris, W. F.
462 (2022). Climate change weakens the impact of disturbance interval on the growth rate of
463 natural populations of venus flytrap. *Ecological Monographs*, 92(4):e1528.

- 464 Merow, C., Bois, S. T., Allen, J. M., Xie, Y., and Silander Jr, J. A. (2017). Climate change both
465 facilitates and inhibits invasive plant ranges in new england. *Proceedings of the National*
466 *Academy of Sciences*, 114(16):E3276–E3284.
- 467 Miller, T. and Compagnoni, A. (2022a). Data from: Two-sex demography, sexual niche
468 differentiation, and the geographic range limits of texas bluegrass (*Poa arachnifera*). *American*
469 *Naturalist, Dryad Digital Repository*,. <https://doi.org/10.5061/dryad.kkwh70s5x>.
- 470 Miller, T. E. and Compagnoni, A. (2022b). Two-sex demography, sexual niche differentiation,
471 and the geographic range limits of texas bluegrass (*poa arachnifera*). *The American*
472 *Naturalist*, 200(1):17–31.
- 473 Morrison, C. A., Robinson, R. A., Clark, J. A., and Gill, J. A. (2016). Causes and consequences
474 of spatial variation in sex ratios in a declining bird species. *Journal of Animal Ecology*,
475 85(5):1298–1306.
- 476 Morrison, S. F. and Hik, D. S. (2007). Demographic analysis of a declining pika *ochotona*
477 *collaris* population: linking survival to broad-scale climate patterns via spring snowmelt
478 patterns. *Journal of Animal ecology*, pages 899–907.
- 479 Nomoto, H. A. and Alexander, J. M. (2021). Drivers of local extinction risk in alpine plants
480 under warming climate. *Ecology Letters*, 24(6):1157–1166.
- 481 O'Connell, R. D., Doak, D. F., Horvitz, C. C., Pascarella, J. B., and Morris, W. F. (2024). Nonlinear
482 life table response experiment analysis: Decomposing nonlinear and nonadditive population
483 growth responses to changes in environmental drivers. *Ecology Letters*, 27(3):e14417.
- 484 Pease, C. M., Lande, R., and Bull, J. (1989). A model of population growth, dispersal and
485 evolution in a changing environment. *Ecology*, 70(6):1657–1664.
- 486 Petry, W. K., Soule, J. D., Iler, A. M., Chicas-Mosier, A., Inouye, D. W., Miller, T. E., and
487 Mooney, K. A. (2016). Sex-specific responses to climate change in plants alter population
488 sex ratio and performance. *Science*, 353(6294):69–71.
- 489 Piironen, J. and Vehtari, A. (2017). Comparison of bayesian predictive methods for model
490 selection. *Statistics and Computing*, 27:711–735.
- 491 Pottier, P., Burke, S., Drobniak, S. M., Lagisz, M., and Nakagawa, S. (2021). Sexual (in) equality?
492 a meta-analysis of sex differences in thermal acclimation capacity across ectotherms.
493 *Functional Ecology*, 35(12):2663–2678.

- 494 Reed, P. B., Peterson, M. L., Pfeifer-Meister, L. E., Morris, W. F., Doak, D. F., Roy, B. A., Johnson,
495 B. R., Bailes, G. T., Nelson, A. A., and Bridgham, S. D. (2021). Climate manipulations
496 differentially affect plant population dynamics within versus beyond northern range limits.
497 *Journal of Ecology*, 109(2):664–675.
- 498 Sanderson, B. M., Knutti, R., and Caldwell, P. (2015). A representative democracy to reduce
499 interdependency in a multimodel ensemble. *Journal of Climate*, 28(13):5171–5194.
- 500 Sasaki, M., Hedberg, S., Richardson, K., and Dam, H. G. (2019). Complex interactions
501 between local adaptation, phenotypic plasticity and sex affect vulnerability to warming
502 in a widespread marine copepod. *Royal Society open science*, 6(3):182115.
- 503 Schwalm, C. R., Glendon, S., and Duffy, P. B. (2020). Rcp8. 5 tracks cumulative co2 emissions.
504 *Proceedings of the National Academy of Sciences*, 117(33):19656–19657.
- 505 Schwinning, S., Lortie, C. J., Esque, T. C., and DeFalco, L. A. (2022). What common-garden
506 experiments tell us about climate responses in plants.
- 507 Sexton, J. P., McIntyre, P. J., Angert, A. L., and Rice, K. J. (2009). Evolution and ecology of
508 species range limits. *Annu. Rev. Ecol. Evol. Syst.*, 40:415–436.
- 509 Smith, M. D., Wilkins, K. D., Holdrege, M. C., Wilfahrt, P., Collins, S. L., Knapp, A. K., Sala,
510 O. E., Dukes, J. S., Phillips, R. P., Yahdjian, L., et al. (2024). Extreme drought impacts have
511 been underestimated in grasslands and shrublands globally. *Proceedings of the National
512 Academy of Sciences*, 121(4):e2309881120.
- 513 Stan Development Team (2023). RStan: the R interface to Stan. R package version 2.21.8.
- 514 Thomson, A. M., Calvin, K. V., Smith, S. J., Kyle, G. P., Volke, A., Patel, P., Delgado-Arias,
515 S., Bond-Lamberty, B., Wise, M. A., Clarke, L. E., et al. (2011). Rcp4. 5: a pathway for
516 stabilization of radiative forcing by 2100. *Climatic change*, 109:77–94.
- 517 Tognetti, R. (2012). Adaptation to climate change of dioecious plants: does gender balance
518 matter? *Tree Physiology*, 32(11):1321–1324.
- 519 Villegas, J., Doak, D. F., García, M. B., and Morris, W. F. (2015). Demographic compensation
520 among populations: what is it, how does it arise and what are its implications? *Ecology
521 letters*, 18(11):1139–1152.
- 522 Welbergen, J. A., Klose, S. M., Markus, N., and Eby, P. (2008). Climate change and the
523 effects of temperature extremes on australian flying-foxes. *Proceedings of the Royal Society
524 B: Biological Sciences*, 275(1633):419–425.

⁵²⁵ Zhao, H., Li, Y., Zhang, X., Korpelainen, H., and Li, C. (2012). Sex-related and stage-dependent
⁵²⁶ source-to-sink transition in *populus cathayana* grown at elevated co₂ and elevated
⁵²⁷ temperature. *Tree Physiology*, 32(11):1325–1338.

Supporting Information

528 S.1 XX

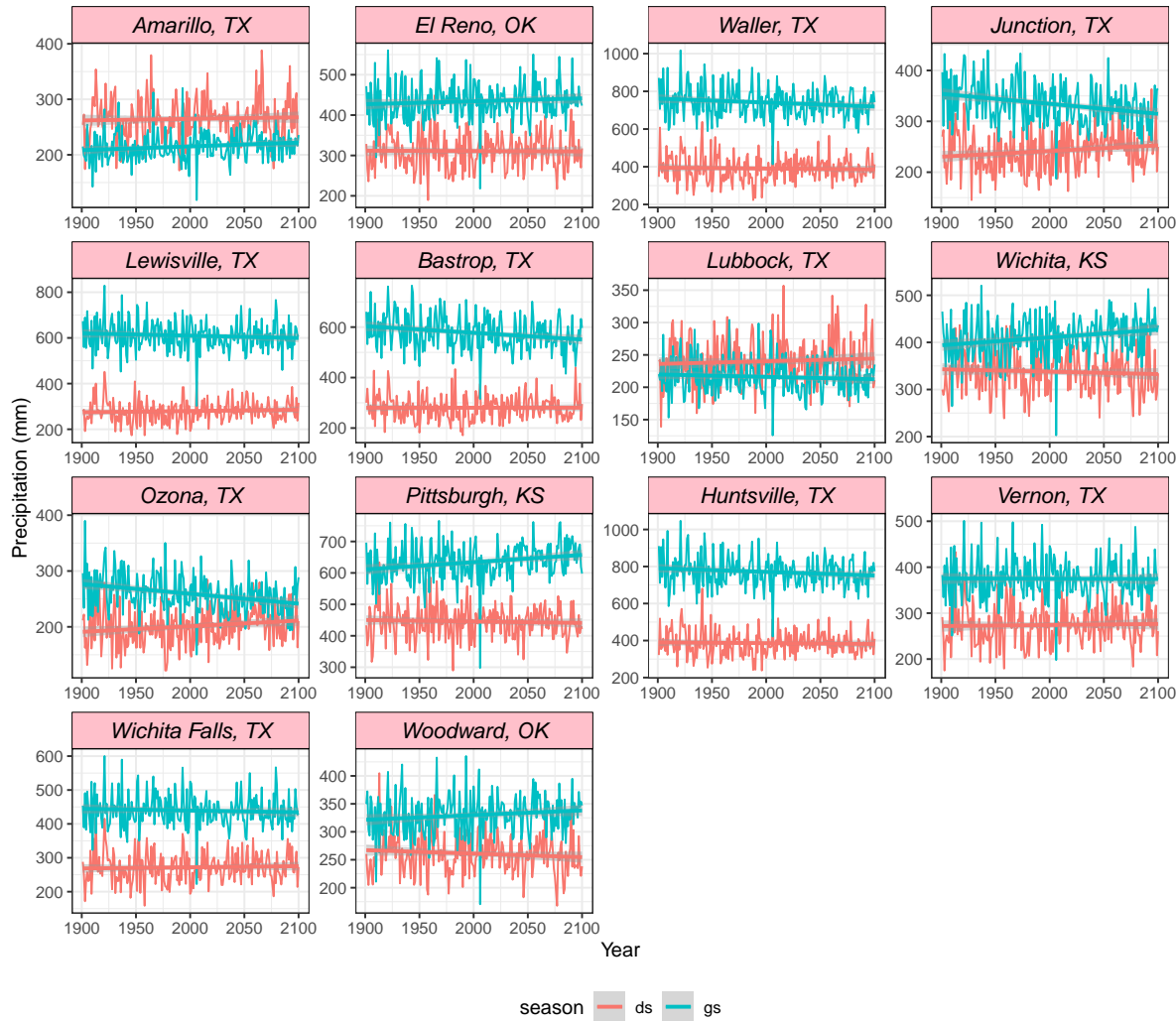


Figure S-1: Precipitation variation accross the study sites from 1990 to 2100

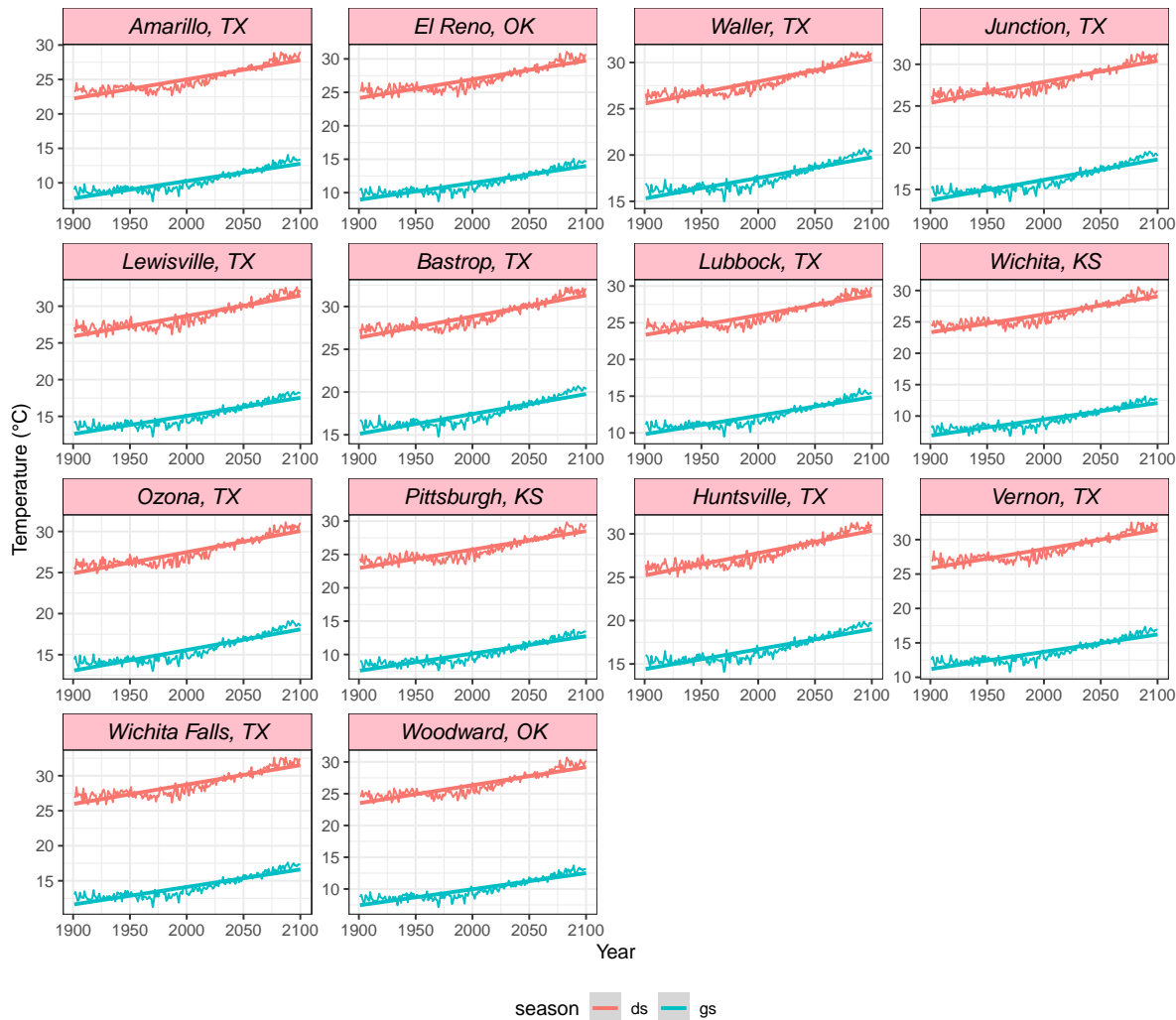


Figure S-2: Temperature variation accross the study sites from 1990 to 2100

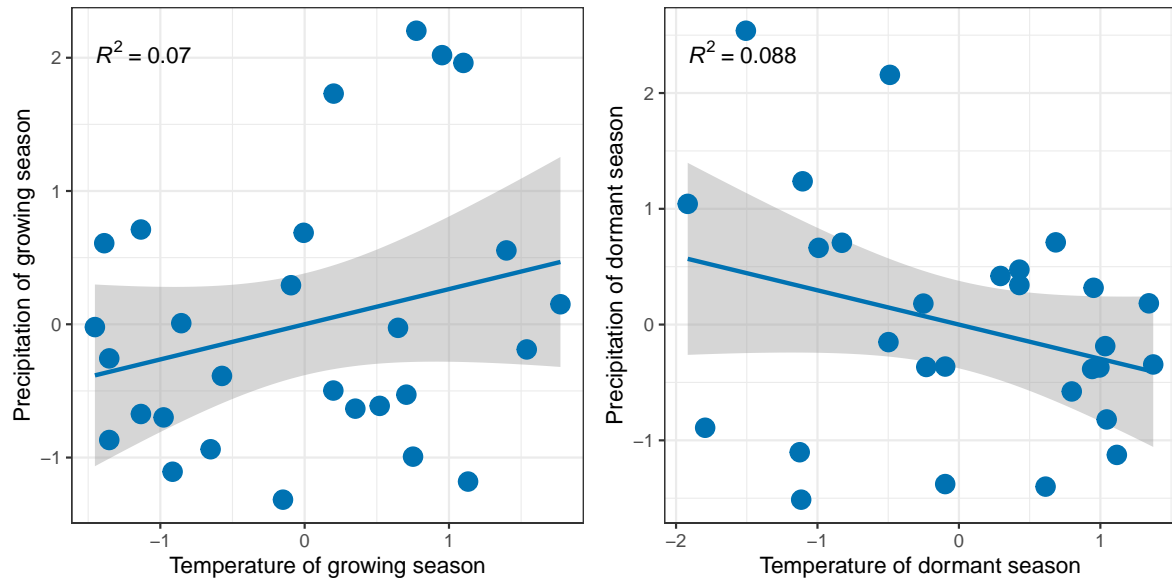


Figure S-3: Relation between precipitation and temperature for each season (growing and dormant). R^2 indicates the value of proportion of explained variance between the temperature and precipitation

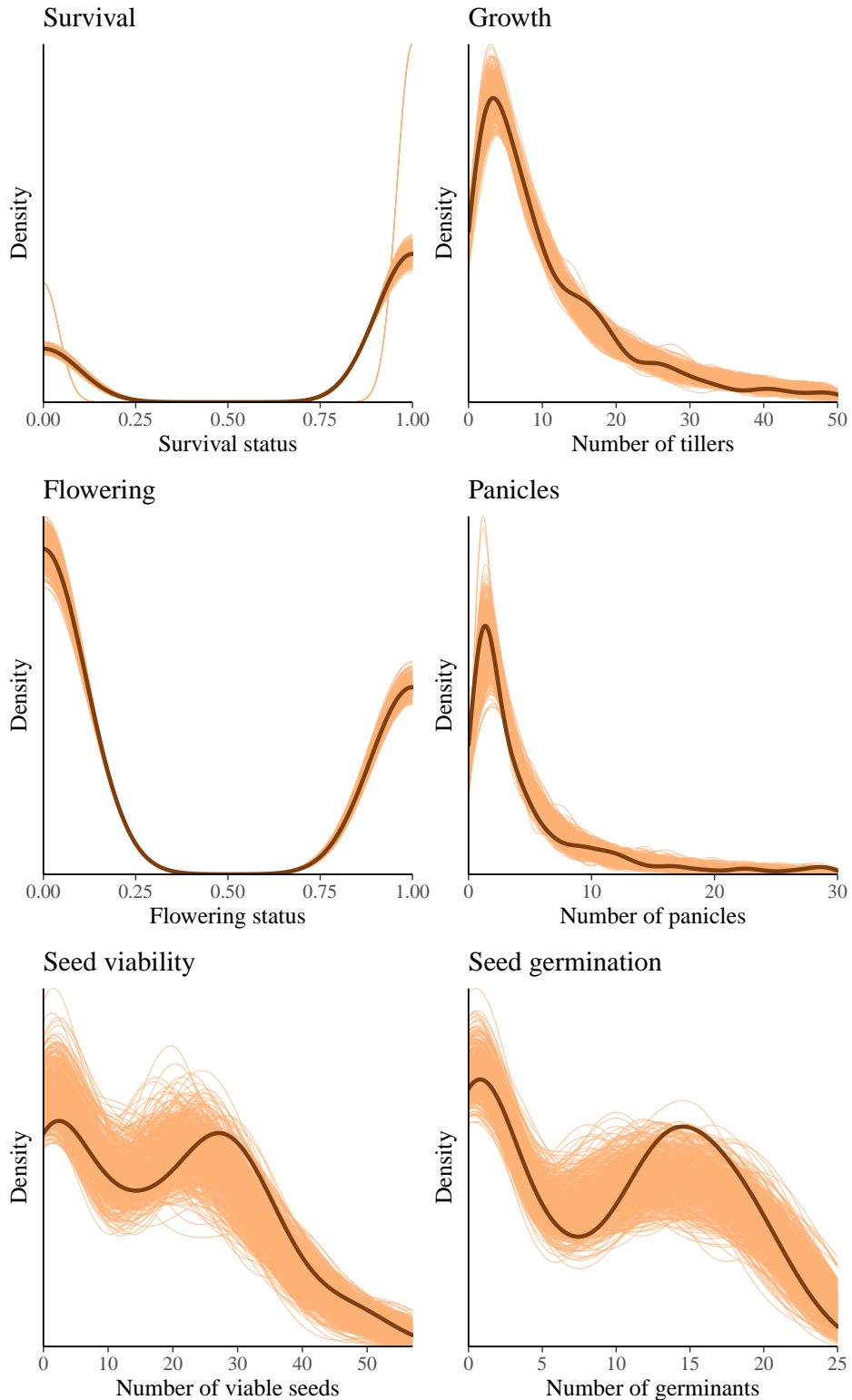


Figure S-4: Consistency between real data and simulated values suggests that the fitted model accurately describes the data. Graph shows density curves for the observed data (light blue) along with the simulated values (dark blue). The first column shows the linear models and the second column shows the 2 degree polynomial models.

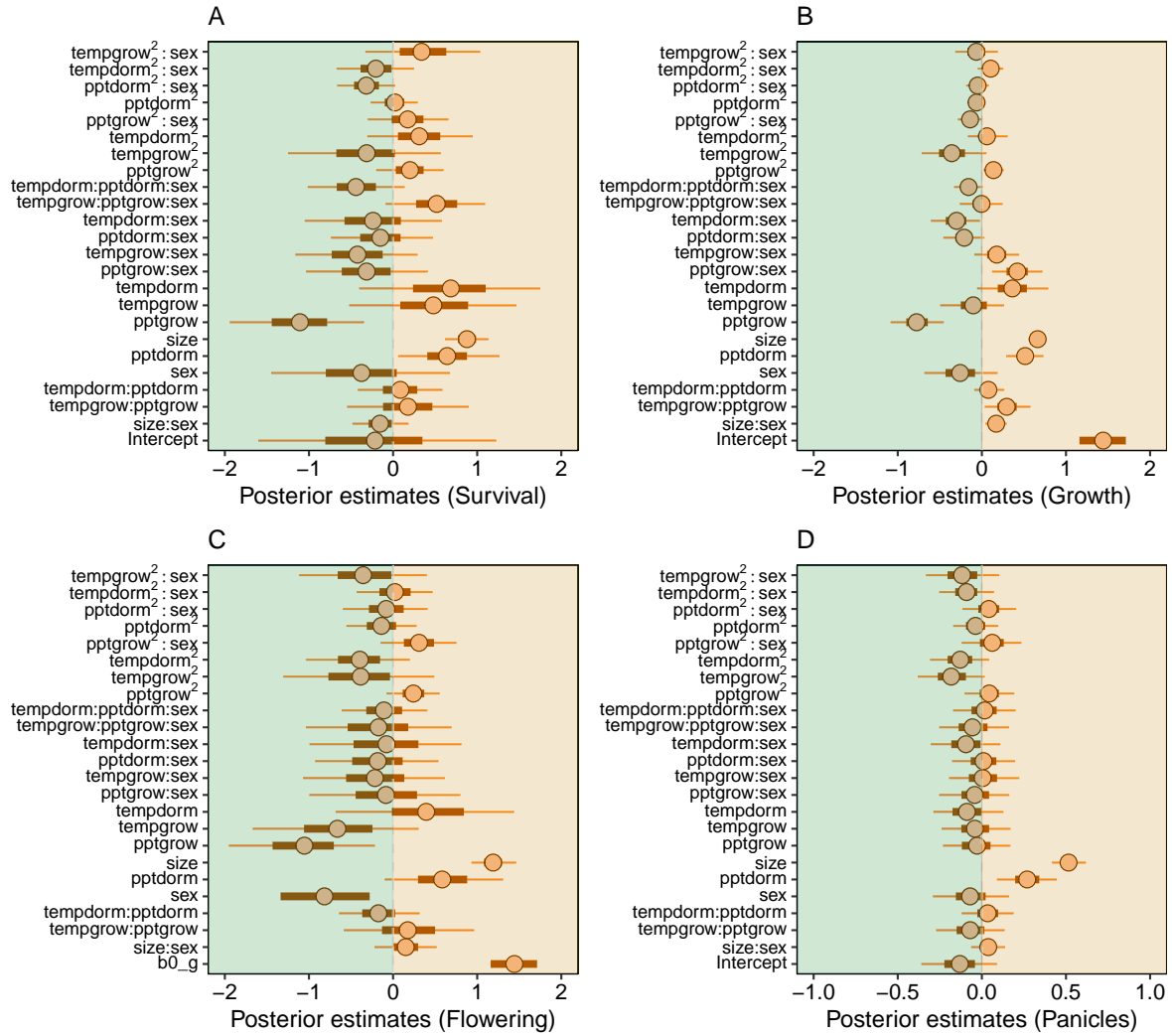


Figure S-5: Mean parameter values and 95% credible intervals for all vital rates.

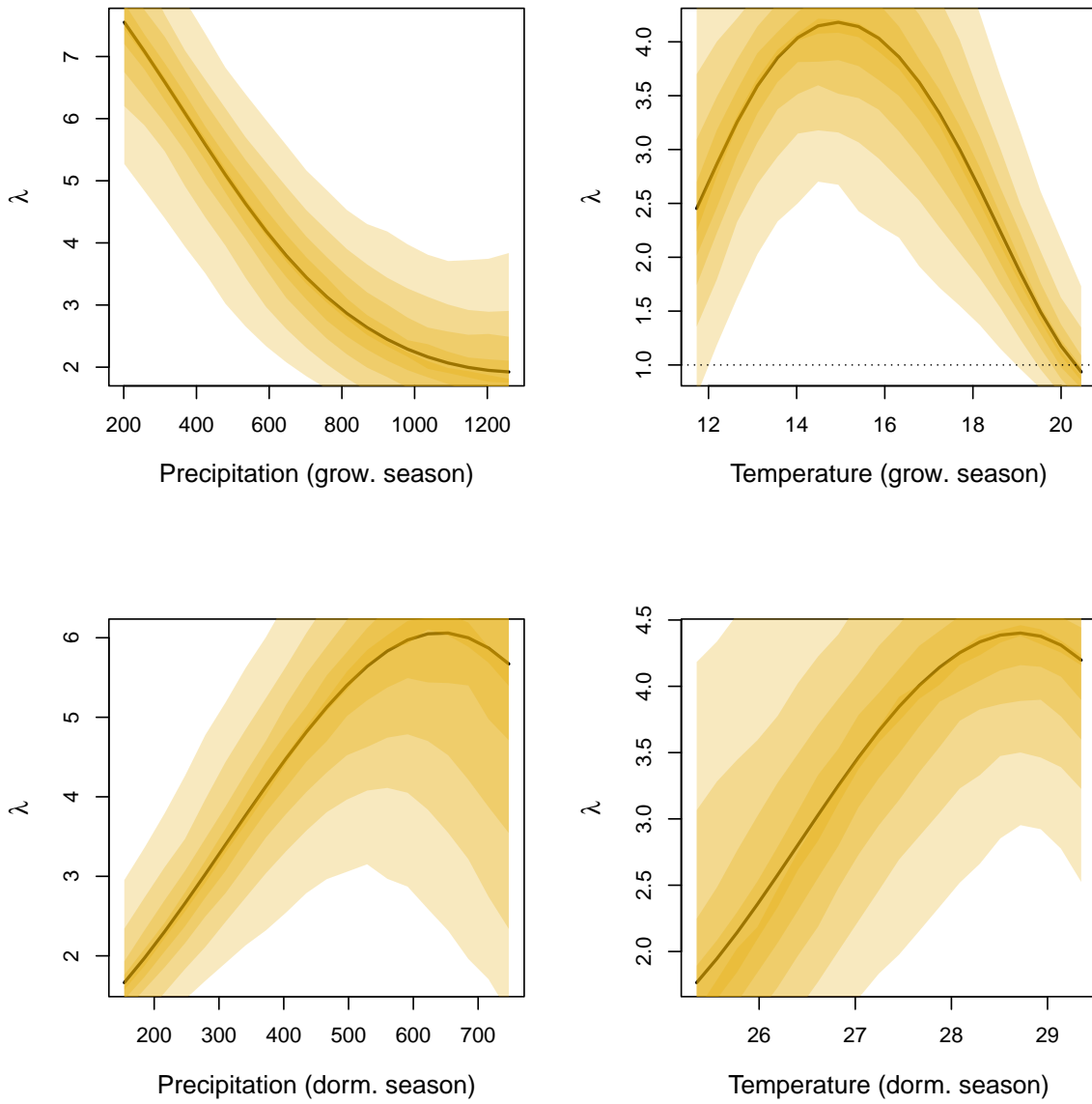


Figure S-6: Population growth rate (λ) as a function of seasonal climate (2016-2017), predicted by the two-sex matrix projection model that incorporates sex-specific demographic responses to climate with sex ratio-dependent seed fertilization. We show the mean posterior distribution of λ in solid lines, and the 5, 25, 50, 75, and 95% percentiles of parameter uncertainty in shaded gold color. The dashed horizontal line indicates the limit of population viability ($\lambda = 1$)

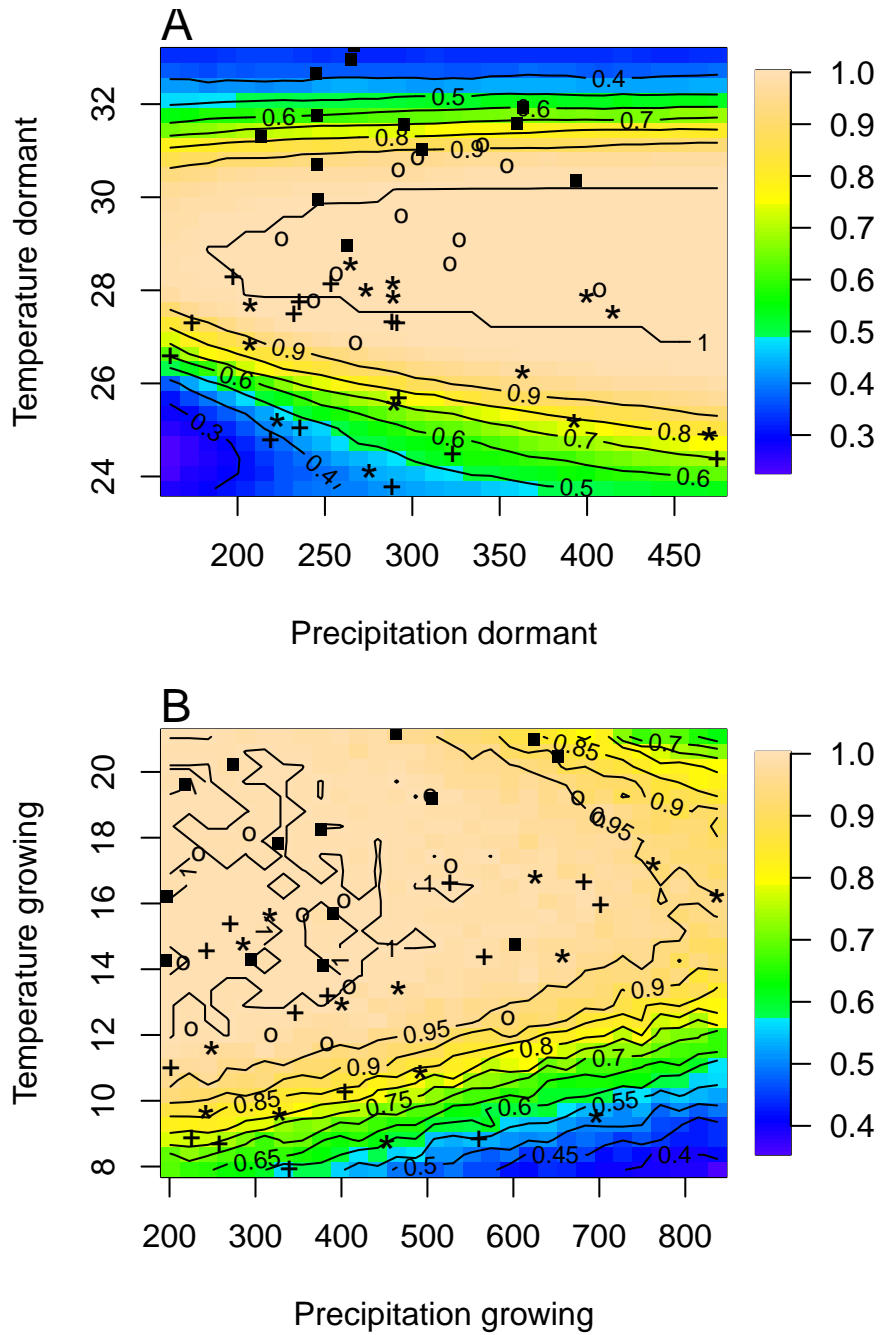


Figure S-7: Predicted niche shift for past, present and future climate conditions based on $\text{Pr} (\lambda \geq 1)$. Niche of dormant season (A), Niche of growing season (B). Contours show predicted probabilities of self-sustaining populations $\text{Pr} (\lambda \geq 1)$ conditional on precipitation and temperature of the dormant and growing season. "+" Past, "*" Current, "o" RCP 45, "." RCP 85

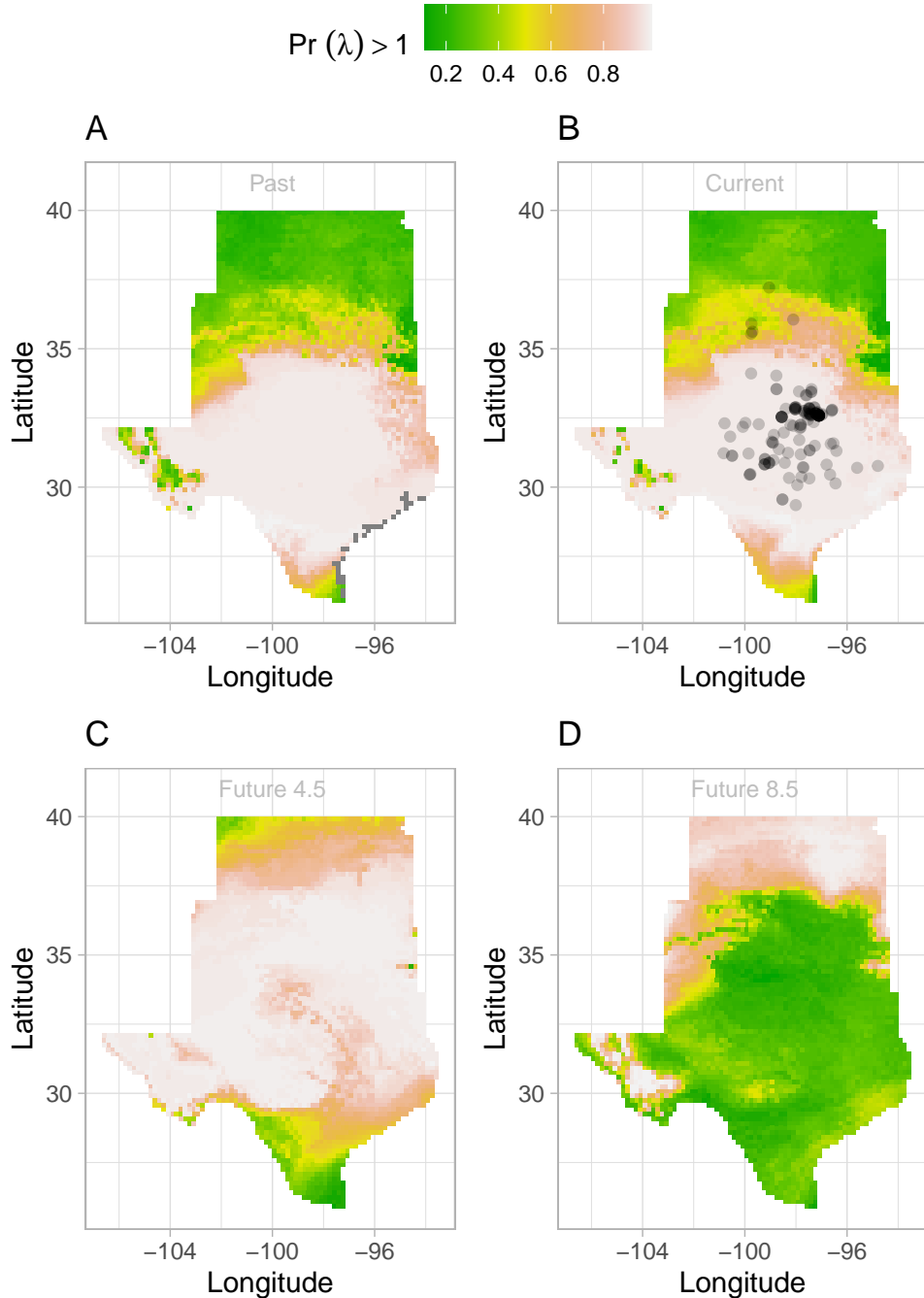


Figure S-8: Past (A), Current (B), Future CMCM (2070–20100) (C and D) predicted range shift based on population growth rate. Future projections were based on the average population growth rate in four GCMs. The black circles on panel B indicate all known presence points collected from GBIF from 1990 to 2019, which corresponds to the current condition in our prediction. The occurrences of GBIFs are distributed in with higher population fitness habitat ($\lambda > 1$), confirming that our study approach can reasonably predict range shifts.

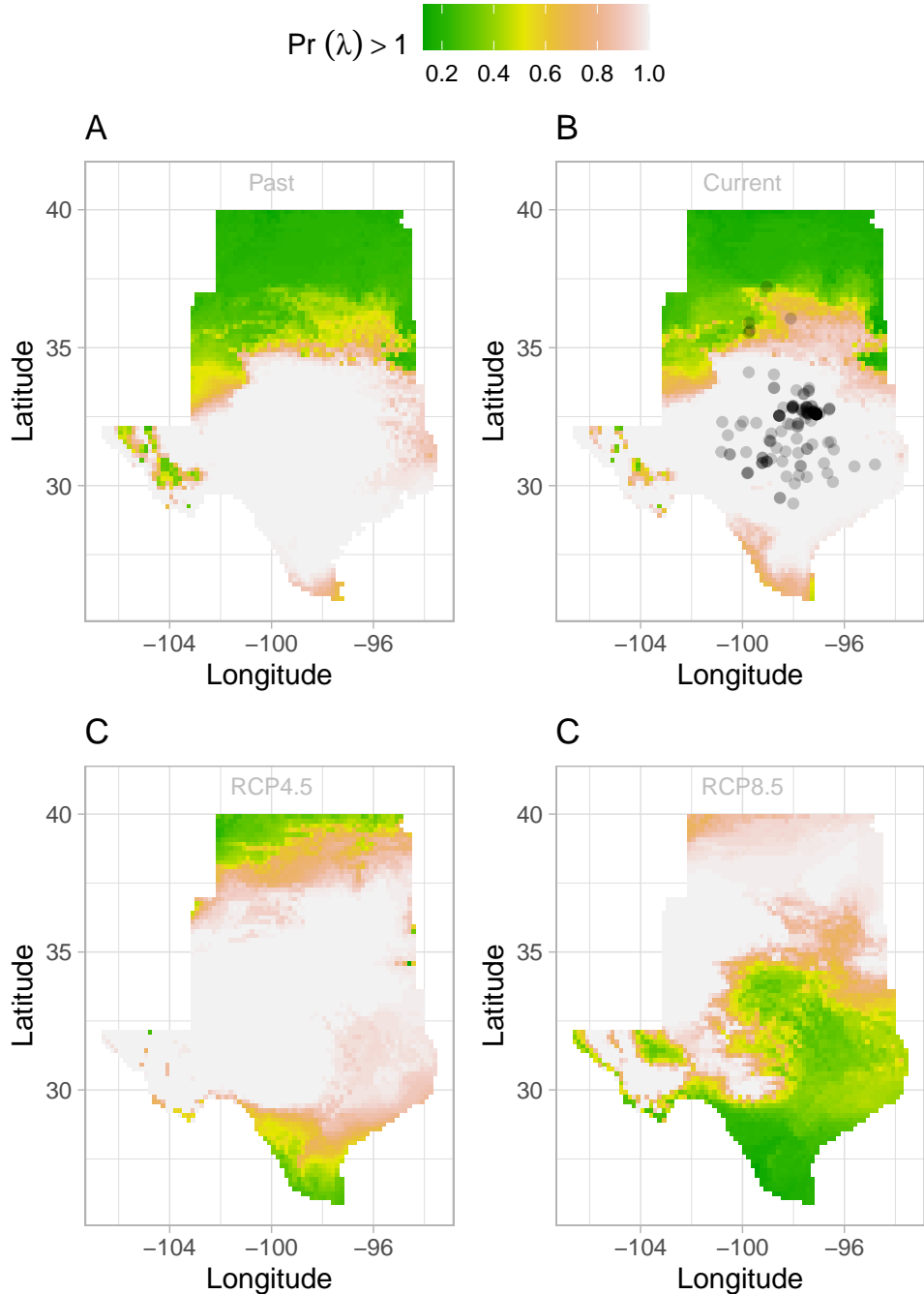


Figure S-9: Past (A), Current (B), Future ACCESS (2070–20100) (C and D) predicted range shift based on population growth rate suing the female dominat model. Future projections were based on the average population growth rate in four GCMs. The black circles on panel B indicate all known presence points collected from GBIF from 1990 to 2019, which corresponds to the current condition in our prediction. The occurrences of GBIFs are distributed inwith higher population fitness habitat ($\lambda > 1$) , confirming that our study approach can reasonably predict range shifts.

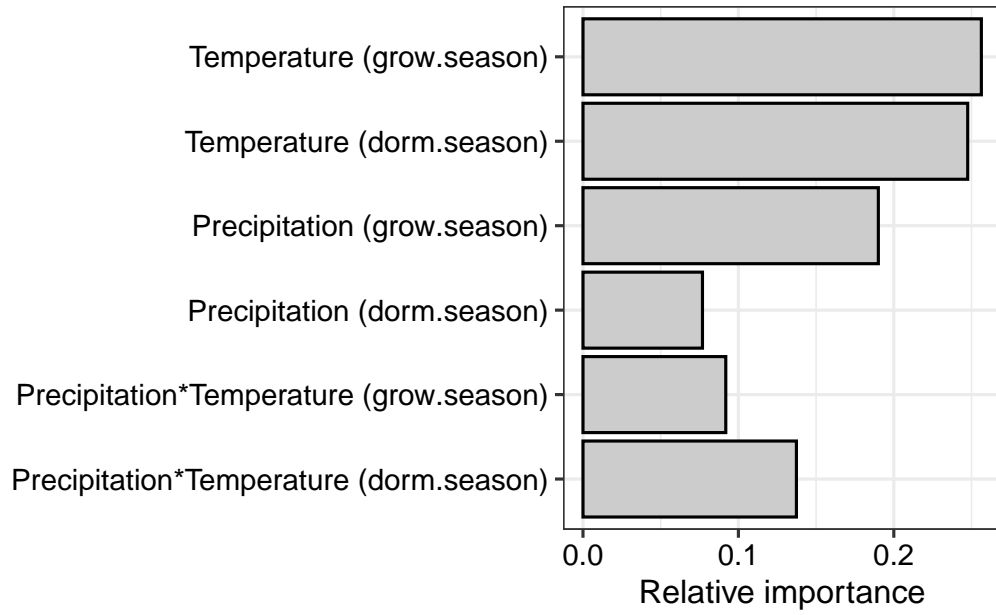


Figure S-10: XXX

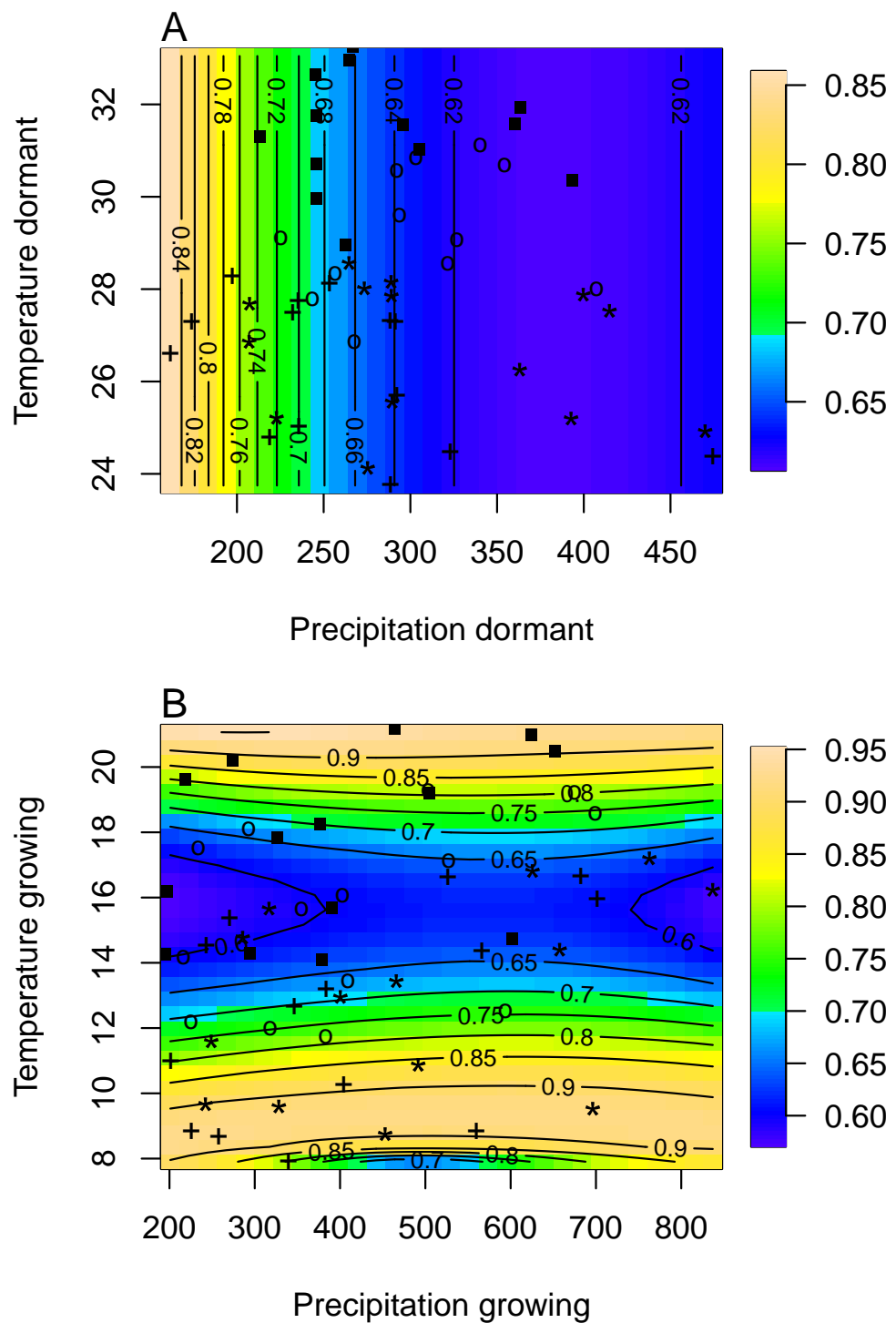


Figure S-11: XXX

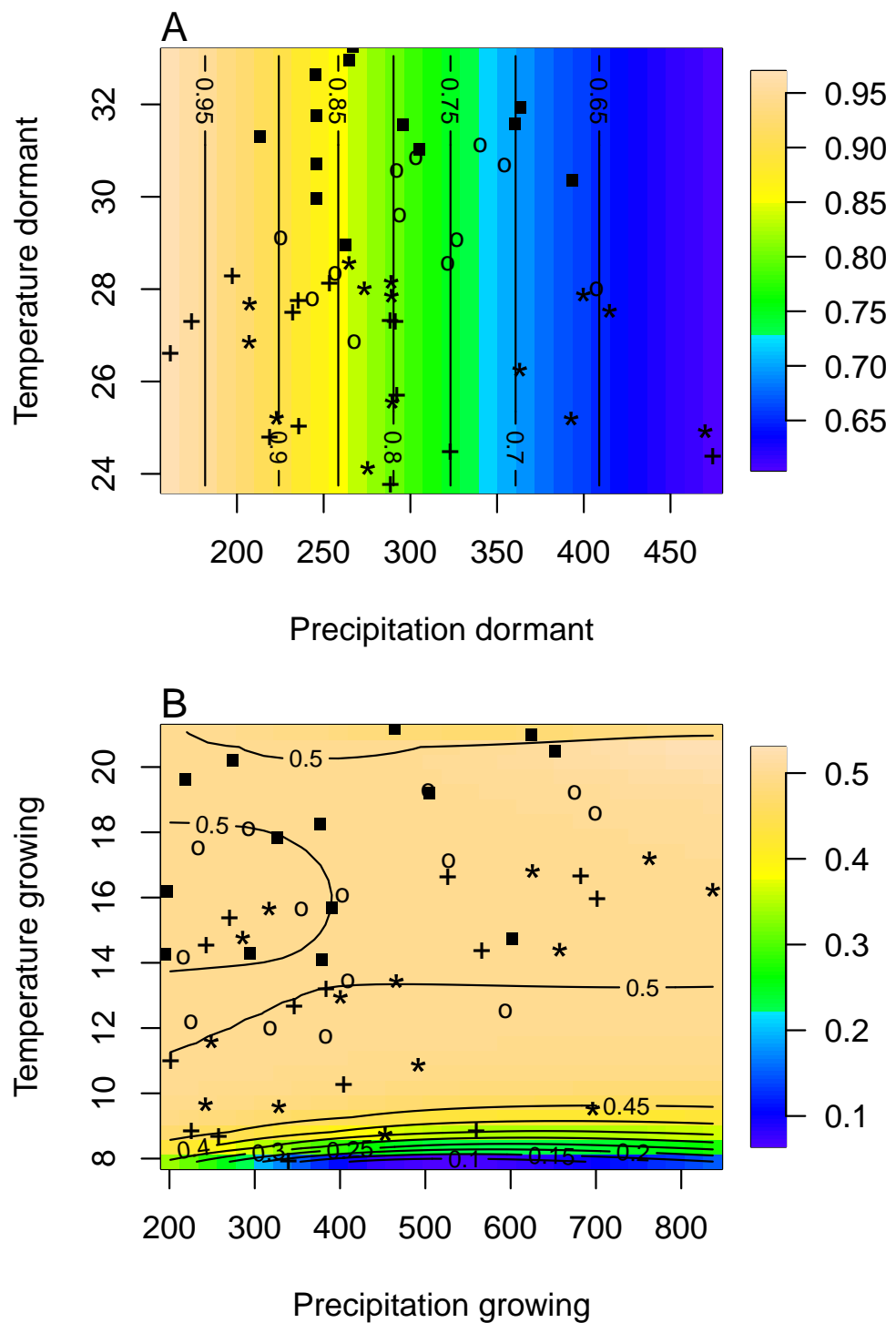


Figure S-12: XXX